

# **Influence of Antimony-Halogen Additives on Flame Propagation**

Valeri I. Babushok<sup>1</sup>, Peter Deglmann<sup>2</sup>, Roland Krämer<sup>3</sup>, Gregory T. Linteris<sup>1</sup>

<sup>1</sup>Engineering Laboratory, National Institute of Standards and Technology; Gaithersburg, MD, USA

<sup>2</sup>BASF SE, Advanced Materials and Systems Research, Ludwigshafen, Germany

<sup>3</sup>BASF SE, Advanced Materials and Systems Research, Shanghai, China

To be submitted to *Combustion Science and Technology*

Key Words: Polymer flammability; material flammability; antimony fire retardant; bromine fire retardant; halogen fire retardant; fire retardant; kinetic model; flame inhibition; antimony trihydride; antimony tribromide

Corresponding author:

Valeri Babushok

National Institute of Standards and Technology

Engineering Laboratory

Gaithersburg, MD 20899

[vbabushok@nist.gov](mailto:vbabushok@nist.gov)

## Influence of Antimony-Halogen Additives on Flame Propagation\*

Valeri I. Babushok, Peter Deglmann, Roland Kraemer, Gregory T. Linteris

### Abstract

A kinetic model for flame inhibition by antimony-halogen compounds in hydrocarbon flames is developed. Thermodynamic data for the relevant species are assembled from the literature, and calculations are performed for a large set of additional species of Sb-Br-C-H-O system. The main Sb- and Br-containing species in the combustion products and reaction zone are determined using flame equilibrium calculations with a set of possible Sb-Br-C-H-O species, and these are used to develop the species and reactions in a detailed kinetic model for antimony flame inhibition. The complete thermodynamic data set and kinetic mechanism are presented. Laminar burning velocity simulations are used to validate the mechanism against available data in the literature, as well as to explore the relative performance of the antimony-halogen compounds. Further analysis of the premixed flame simulations has unraveled the catalytic radical recombination cycle of antimony. It includes (primarily) the species Sb, SbO, SbO<sub>2</sub>, and HOSbO, and the reactions: Sb+O+M=SbO+M; Sb+O<sub>2</sub>+M=SbO<sub>2</sub>+M; SbO+H=Sb+OH; SbO+O=Sb+O<sub>2</sub>; SbO+OH+M=HOSbO+M; SbO<sub>2</sub>+H<sub>2</sub>O=HOSbO+OH; HOSbO+H=SbO+H<sub>2</sub>O; SbO+O+M=SbO<sub>2</sub>+M. The inhibition cycles of antimony are shown to be more effective than those of bromine, and intermediate between the highly effective agents CF<sub>3</sub>Br and trimethylphosphate. Preliminary examination of a Sb/Br gas-phase system did not show synergism in the gas-phase catalytic cycles (i.e., they acted essentially independently).

**Keywords:** antimony fire retardant, bromine fire retardant, synergism, flame inhibition, antimony tribromide

### 1. Introduction

Antimony trioxide, together with organochlorine and organobromine compounds, is a widely used fire retardant additive in commodity polymers. This application represents the largest commercial use of antimony (as well as of bromine). The fire retardant action is believed to occur in the gas phase (Fenimore and Martin, 1966b, Fenimore and Martin, 1966a, Fenimore and Jones, 1966, Fenimore and Martin, 1972). Yet in spite of the long use and many studies of antimony-bromine systems as fire retardants, for example (Hastie and McBee, 1975, Khalturinskii and Rudakova, 2008, Lewin, 1999, Lewin, 2001, Linteris, 2002, Salmeia et al., 2015, Weil, 2011, Weil and Levchik, 2007), there have been few fundamental studies describing the gas phase inhibition mechanism by antimony and its synergetic effect when combined with chlorine or bromine. Unlike most other gas-phase active flame inhibitors, there are no kinetic or thermodynamic models for antimony flame inhibition, and consequently, there has been no simulation or analysis of those systems. Due to health, environmental, and other concerns, there is motivation in industry to find

alternatives to the antimony-bromine system for fire retarding high-volume commodity polymers. It is believed that a detailed understanding of the flame inhibition mechanism of the antimony-bromine system will allow more efficient use of existing and new formulations, as well as development of alternative compounds.

There have been a few experimental studies of the inhibition effectiveness of antimony compounds for gas phase flames. In seminal work, Lask and Wagner (Lask and Wagner, 1962) examined the reduction in laminar burning velocity (using nozzle burners) and flammability limits with addition of a wide variety of compounds (including the elements: P, Br, Cl, Ti, Sn, Ge, Fe) to premixed hexane- and hydrogen-air flames. In related unpublished work (as cited in (McHale, 1969)) they did measurements with  $\text{SbCl}_3$  and found it to be about 15 % less effective than the highly effective agents  $\text{SnCl}_4$ ,  $\text{TiCl}_4$ , and  $\text{POCl}_3$ , which, based on experiments in premixed methane-air flames for  $\text{SnCl}_4$  and  $\text{CF}_3\text{Br}$  (Linteris et al., 2002), implies that  $\text{SbCl}_3$  is about 2.6 times as effective as  $\text{CF}_3\text{Br}$ . Miller et al. (Miller et al., 1963) studied the influence of antimony pentachloride on hydrogen-air burning velocities, and found it to be about five times as effective as  $\text{CF}_3\text{Br}$  for rich flames. In molecular-beam mass spectrometry experiments, Hastie et al. (Hastie, 1973a, Hastie, 1973b, Hastie and McBee, 1975) determined the flame structure of methane-air flames inhibited by  $\text{SbCl}_3$  and  $\text{SbBr}_3$ . All these studies demonstrated that antimony compounds themselves are effective flame inhibitors.

The goal of the present work is to develop a kinetic model of flame inhibition by antimony-bromine compounds and use it to study the influence of Sb-Br compounds on premixed flames. To this end we have performed calculations of thermodynamic properties for a large set Sb-Br-C-H-O species, and use these in combustion equilibrium calculations for methane-air flames doped by Sb- and Br-containing additives. Based on these calculations and the experimental results for similar systems in the literature, a limited set of relevant species is suggested for initial kinetic model generation. This model is used to simulate the influence of several Sb-containing compounds ( $\text{SbH}_3$ ,  $\text{SbCl}_3$ ,  $\text{SbCl}_5$ ,  $\text{SbBr}_3$ ,  $\text{ClSbO}$ ,  $\text{BrSbO}$ ) on the burning velocity of methane-air flames; for comparison, data for the inhibition effectiveness of bromine- ( $\text{HBr}$ ) and phosphorus-containing (TMP, trimethyl phosphate) additives are also presented. The mechanism of inhibition by antimony compounds is studied; and finally, a simple binary system with Sb- and Br-containing species is simulated to explore synergism in the gas phase.

## 2. Kinetic models and modeling procedure

Although it is most desirable to test the Sb flame inhibition model using data for a simple Sb-containing hydrocarbon, there are no such data in the literature for comparison. Data only exist for H<sub>2</sub>-air flames inhibited by SbCl<sub>5</sub> (Miller et al., 1963) and hexane-air flames inhibited by SbCl<sub>3</sub> (McHale, 1969). Hence, in order to test the Sb mechanism against experimental data, kinetic models are required for Sb/Cl flame inhibition in hydrocarbon-air flames (hydrogen-air, hexane-air), as well as for the combined Sb/Br flame inhibition (present work), and methane-air flames (for exploratory simulations). In total, the inhibiting species of interest (for which mechanisms are required) in the present work are: SbH<sub>3</sub>, SbBr<sub>3</sub>, BrSbO, SbCl<sub>3</sub>, SbCl<sub>5</sub>, ClSbO, Sb<sub>4</sub>O<sub>6</sub>, CF<sub>3</sub>Br, HBr and TMP (trimethyl phosphate). The sources of these required models are described below.

For methane and hydrogen flames, the kinetic model Grimech-3.0 is employed (Smith et al., 2000). For hexane, the C1–C4 model of Wang et al (Wang et al., 2007) is used as a basis, as in our previous work (Babushok et al., 2012), with the work of Burcat et al. (Burcat et al., 1996) providing decomposition pathways down to C1-C4 species. The bromine-species reactions (Br-C-H-O) are extracted from a recently-developed mechanism for C<sub>3</sub>H<sub>2</sub>F<sub>3</sub>Br flame inhibition (Babushok et al., 2015). The chlorine-species reactions (Cl-C-H-O) are extracted from recent work for C<sub>2</sub>H<sub>2</sub>F<sub>3</sub>Cl<sub>2</sub> flame inhibition (Babushok et al., 2014). Since P and Sb are in the same periodic group, simulations with a phosphorus compound are useful for comparison. Trimethylphosphate (TMP) is used for these comparisons, since experimental, modeling, and validation studies have been performed for it. To model phosphorus-species flame inhibition by TMP, the kinetic model of Jayavera et al. is used (Jayaweera et al., 2005). Development of the kinetic model for antimony-bromine compounds is described below.

Note that Sb<sub>4</sub>O<sub>6</sub>, antimony oxide, is used as a model compound for test calculations and for comparison purposes. Sb<sub>4</sub>O<sub>6</sub> is a product of antimony combustion in air for a low temperature range. It is known that evaporation of antimony trioxide, Sb<sub>2</sub>O<sub>3</sub> leads to Sb<sub>4</sub>O<sub>6</sub> in a gas phase (Asryan et al., 2004, Behrens and Rosenblat, 1973, Kunkel et al., 2014). The kinetics of the decomposition of Sb<sub>4</sub>O<sub>6</sub> in the flame is represented by a simplified, overall reaction down to the Sb-containing species considered in the kinetic model. It is assumed that the decomposition details have a relatively small impact on the burning velocity of inhibited flames, as discussed previously (Linteris et al., 2000). The Chemkin set of programs of Sandia Laboratory is used for the

combustion equilibrium calculations and for modeling laminar premix flames. Typical values of grad and curve parameters are 0.12 and 0.27, respectively, for the calculations.

### 3. Results and Discussion

#### 3.1. Sb-, Br-, and Cl-containing species list and thermochemical data

A starting list of compounds for inclusion in the model was developed from consideration of possible antimony species containing Br, Cl, H, C, and O. Resources for this list include the CAS registry (SciFinder) and thermodynamic databases (Goos et al., 2012, Gurvich et al., 1993). Further refinement was performed based on calculated thermodynamic data (Skulan et al., 2006), analogy with the phosphorus flame inhibition model (Jayaweera et al., 2005), mass-spectrometry (Hastie, 1973a, Hastie, 1973b, Hastie et al., 1986, Hastie and McBee, 1975) and spectroscopic (Farber and Srivastava, 1975) species measurement in flames, and other species observed experimentally. The list is presented in **Error! Reference source not found.** In this initial mechanism, the list was constrained to species with one antimony atom (assuming that in flame reaction zone, the antimony species will have decomposed to those with only one Sb atom). As described below, thermodynamic calculations indicate a relatively high concentration of Sb atom at equilibrium; therefore, some recombination of Sb atoms can be expected and the species Sb<sub>2</sub> was included.

As indicated in **Error! Reference source not found.**, thermodynamic data were obtained or calculated for the heat of formation  $\Delta H_f$ , entropy  $S$ , and specific heat  $C_p$  at 298 K. Literature data from Burcat et al. (Goos et al., 2012), Skulan et al. (Skulan et al., 2006) and the IVTANTHERMO database (Gurvich et al., 1993) were used when available. For the remaining species of interest, thermodynamic data were calculated at the CCSD(T)/aug-cc-pVTZ level of theory based on structures optimized at the BP86/SV(P) level as implemented in the program package TURBOMOLE (Ahlrichs et al., 1989). This was done using standard protocols for thermodynamic function calculations like rigid rotor and harmonic oscillator. Consideration of relativistic effects by ECP (as implemented in TURBOMOLE) was performed (with no spin-orbit coupling). Based on the calculated properties, data in CHEMKIN format (polynomials) were generated, as presented in the Supplementary Materials.

#### 3.2. Flame equilibrium calculations

In order to estimate the relative potential contribution of the different species in **Error! Reference source not found.** at flame temperatures, combustion equilibrium calculations were performed (constant pressure, constant enthalpy or temperature) using the Sandia EQUIL program (Reynolds, 1986). The initial conditions are methane-air mixtures at 298 K, 1 bar, to which the antimony compound ( $\text{SbH}_3$ ,  $\text{SbBr}_3$ ) is added at a volume fraction (in the entire mixture) of 0.25 %. For the additive  $\text{SbH}_3$ , Figure 1 shows the equilibrium volume fraction for each of the species in **Error! Reference source not found.** (for those having a peak value above  $10^{-11}$ ) as a function of temperature. Figure 2 shows the results for  $\text{SbBr}_3$  addition as a function of combustion temperature, while Figure 3 shows the results as a function of the initial equivalence ratio of the methane-air flame. As Figure 1 and Figure 3 show, the main Sb-containing species, in approximate order of relative abundance, are  $\text{HOSbO}$ ,  $\text{Sb}$ ,  $\text{SbO}$ ,  $\text{Sb(OH)}_3$ ,  $\text{Sb(OH)}_2$ ,  $\text{SbOH}$ ,  $\text{SbH}$ ,  $\text{HSbO}$ ,  $\text{SbO}_2$ , and  $\text{HOSbO}_2$ . To determine the influence of agent loading on equilibrium product distribution, calculations (not shown here) were also performed varying the initial antimony species (in this case,  $\text{SbH}_3$ ) volume fraction from 0.1 to 3 %. The results show an approximate linear increase in all product species concentrations, with no major changes in the product distributions. For  $\text{SbBr}_3$  addition (also at a volume fraction of 0.25 %), Figure 2 shows that the major equilibrium species in the methane-air flame are:  $\text{HBr}$ ,  $\text{Br}$ ,  $\text{HOSbO}$ ,  $\text{BrSbO}$ ,  $\text{Sb}$ ,  $\text{SbO}$ ,  $(\text{OH})_2\text{SbBr}$ ,  $\text{Br}_2$ ,  $(\text{HO})\text{SbBr}$ ,  $\text{SbBr}$ ,  $\text{BrOH}$ ,  $\text{BrO}$ ,  $\text{SbBr}_3$ ,  $\text{SbBr}_2$ , and  $(\text{OH})\text{SbBr}_2$ . Based on these equilibrium calculations and the results for the similar phosphorus inhibition mechanism, the following species were adopted for the first iteration of the kinetic model of antimony species:  $\text{Sb}$ ,  $\text{SbO}$ ,  $\text{SbO}_2$ ,  $\text{SbO}_3$ ,  $\text{HOSbO}$ ,  $\text{HOSbO}_2$ ,  $\text{Sb}_2$ ,  $\text{SbOH}$ , and  $\text{SbH}$ . To model the behavior of  $\text{SbBr}_3$ ,  $\text{SbCl}_3$  and  $\text{SbCl}_5$  the following species were additionally included:  $\text{SbBr}_3$ ,  $\text{SbBr}_2$ ,  $\text{SbCl}_5$ ,  $\text{SbCl}_4$ ,  $\text{SbCl}_3$ ,  $\text{SbCl}_2$ ,  $\text{SbCl}$ ,  $\text{ClSbO}$ ,  $\text{SbBr}$ , and  $\text{BrSbO}$ .

The present equilibrium calculations for antimony-containing species can be compared with similar calculation for phosphorus-containing compounds. For the antimony system, the results show a high concentration of Sb atoms, while  $\text{SbO}$  and  $\text{HOSbO}$  dominate as the main oxygenated antimony species. This is in a contrast to phosphorus-containing inhibitors for which the dominant gas-phase oxygenated species are  $\text{PO}_2$ ,  $\text{HOPO}$  and  $\text{HOPO}_2$ , and P atom is not important. The equilibrium concentration of  $\text{HOSbO}_2$  is substantially less than  $\text{HOSbO}$  implying that inhibition chemistry should be dominated by the  $\text{HOSbO}$  species. This is the opposite of

phosphorus inhibition chemistry where both HOPO and HOPO<sub>2</sub> species are important, and participate in two scavenging cycles: PO<sub>2</sub> <=> HOPO and PO<sub>2</sub> <=>HOPO<sub>2</sub>.

Note that experimental results (Farber and Srivastava, 1975, Hastie, 1973a) detected Sb atom, SbO, HOSbO<sub>2</sub>, OSb(OH)<sub>3</sub> and Sb<sub>4</sub>O<sub>6</sub> in the flame reaction zone and combustion products of methane-air and hydrogen-air flames. The species Sb<sub>4</sub>O<sub>6</sub> species was observed in the preheat zone of a methane-air flame (Hastie, 1973a). We believe that the significant concentrations of OSb(OH)<sub>3</sub> and HOSbO<sub>2</sub> observed in the experiments of Farber and Srivastava (Farber and Srivastava, 1975) are the result of post-flame reactions during the quenching process with the additional mixing with the surrounding air.

### 3.3. Kinetic model of inhibition by antimony-containing compounds

To our knowledge there are no available gas phase kinetic models which include Sb-chemistry, and a review of the literature shows that elementary rate data for reactions of Sb-containing stable species and radicals are practically absent. A list of plausible reactions with Sb-, Br- and Cl-containing species was considered. They include the decomposition reactions of SbH<sub>3</sub>, SbBr<sub>3</sub>, SbCl<sub>3</sub> and SbCl<sub>5</sub>, reactions of HOSbO, HOSbO<sub>2</sub>, BrSbO and ClSbO and its products (Sb, SbO, SbO<sub>2</sub>, SBO<sub>3</sub>, SbH, SbH<sub>2</sub>,SbOH, SbBr, SbBr<sub>2</sub>, Sb<sub>2</sub>) with the important radicals (H, OH, O, Br, Cl, CH<sub>3</sub>, HCO, HO<sub>2</sub>), the main hydrocarbon species (CH<sub>4</sub>, C<sub>2</sub>H<sub>6</sub>, CH<sub>2</sub>O), and with the bromine- and chlorine-containing species. Based on thermochemical considerations and estimation of species equilibrium concentrations, this list was reduced to that in Table 2. It contains 179 reactions with 16 Sb/Br-containing species (Sb-Br system), which are combined with the Grimech 3.0 model for methane oxidation, and the CF<sub>3</sub>Br flame inhibition kinetic model (Babushok et al., 2015) for the bromine-species part of the mechanism. The antimony-chlorine kinetic sub-model is presented in the Supplemental Material. Most of the rate constants are estimated based on analogy and using empirical correlations.

As a first step for validating a kinetic mechanism, it is useful to have burning velocity data for inhibited flames for comparison with calculated values. Unfortunately, despite the widespread use of antimony as a fire retardant, there are practically no available experimental data on the effects of Sb-C-H-O compounds on air/hydrocarbon flames for comparison with model predictions. As described above, Miller et al. have provided experimental data (intended for screening purposes)(Miller et al., 1963), of the effect of numerous flame inhibitors on the burning

velocity of hydrogen-air flames measured using the total area method with conical premixed flame (Andrews and Bradley, 1972). Using their data, Figure 4 shows the measured and predicted burning velocity of a hydrogen-air flame (298 K, 1 bar, equivalence ratio of 1.75) with added  $\text{SbCl}_5$ . Although there is large scatter in the experimental data, the agreement appears to be reasonable. Other available data include the unpublished work of Lask and Wagner (cited in (McHale, 1969)) described above, for stoichiometric premixed n-hexane-air flames (modelled as 298 K, 1 bar) with added  $\text{SbCl}_3$ . As with the other inhibitors of the study, the data are reported as the quantity of  $\text{SbCl}_3$  required to reduce the burning velocity of the flames by 30 %. The numerically calculated volume fraction for this level of flame inhibition is 0.18 %, which compares reasonably well to the experimental value (0.22 %).

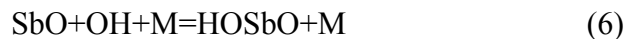
### **3.4. Burning velocity simulations, mechanism of flame inhibition by antimony**

The influence of inhibitor concentration on the burning velocity of laminar hydrocarbon-air flames is often used as a metric for flame inhibition effectiveness. For comparison purposes, Figure 5 shows the calculated burning velocity of stoichiometric methane-air flames with added  $\text{SbH}_3$ ,  $\text{SbBr}_3$ ,  $\text{SbCl}_3$ ,  $\text{Sb}_4\text{O}_6$ ,  $\text{BrSbO}$ , and  $\text{ClSbO}$ , as well as for the more thoroughly studied (and validated) agents  $\text{CF}_3\text{Br}$ ,  $\text{HBr}$  and  $\text{TMP}$  ( $\text{PO}(\text{OCH}_3)_3$ ). Using the current mechanism,  $\text{SbH}_3$  is less effective than the phosphorus compound ( $\text{TMP}$ ), but more effective than bromine containing compounds. As with most flame inhibitors, the marginal reduction in burning velocity decreases as the volume fraction of agent increases (saturation of the inhibition effect (Noto et al., 1998)). At relatively small additive concentrations, the burning velocity reductions of different antimony compounds are relatively close to each other, and close to that of antimony itself (for which data are not shown, but which is the most effective moiety of antimony compounds). Addition of Br atoms to the antimony-containing compound increases the inhibition effectiveness significantly, proportional to the number of Br atoms; Cl addition provides a significant but smaller effect, consistent with previous findings for halogen inhibition (Dixon-Lewis and Simpson, 1977, Westbrook, 1982, Babushok and Tsang, 2000). With the present kinetic mechanism, the modeling results show that for a 10 % reduction in burning velocity (a common metric), Sb-containing compounds (e.g.,  $\text{Sb}_4\text{O}_6$ ) are approximately 3 and 4.3 times more effective than  $\text{CF}_3\text{Br}$  and  $\text{HBr}$ , respectively.



For a methane-air flame with SbH<sub>3</sub> added at a volume fraction of 0.2 %, Figure 6 shows the volume fractions of major species of interest as a function of position in flame. Concentrations of the species SbH<sub>2</sub> and SbH, which are intermediates during decomposition of SbH<sub>3</sub>, are small as a result of their high reactivity. The species HOSbO is present at the highest volume fraction in the flame (around 0.001), existing at super equilibrium levels in the preheat zone, and then approaches equilibrium. The species SbO forms slightly later in the preheat zone, is also present at super-equilibrium levels (about 10x), and then decays towards equilibrium concentrations. The species Sb forms still later, and is sub-equilibrium throughout. The dips in the concentrations of these species at the location of peak radical concentration (flame coordinate of 0.05 cm to 0.1 cm) are related to their consumption in the catalytic radical recombination cycles described below. The volume fraction of another important species in the cycle, SbO<sub>2</sub>, is approximately one to two orders of magnitude smaller than that of SbO as a result of relatively high rates of its conversion to HOSbO.

Figure 7 shows the reaction pathways of SbH<sub>3</sub> decomposition and the fate of antimony species in the flame reaction zone. In the figure, arrows connect the reactants and products of a reaction; the species next to the arrow is the reaction partner, and the number adjacent is the fraction (in %) of the overall consumption rate of the first reactant in that reaction. No reaction partner denotes a unimolecular decomposition reaction; no fraction indicates nearly all of the species goes through that reaction pathway. SbH<sub>3</sub> is consumed primarily through a decomposition reaction, and also via its reaction with radicals (H, OH), to form SbH<sub>2</sub>. The SbH<sub>2</sub> radical and its product, SbH, are mostly consumed through decomposition reactions and via reactions with radicals, forming Sb atom at the end of decomposition sequence. The Sb atom, along with the other intermediate species SbO, SbO<sub>2</sub> and HOSbO, form the sequence of reactions depicted in Figure 7:





As the figure shows, there are multiple catalytic radical scavenging cycles. The simplest is the binary cycle  $\text{Sb} \rightleftharpoons \text{SbO}$  via reactions (1), (4), and (5), while a similar cycle  $\text{SbO} \rightleftharpoons \text{HOSbO}$  via reactions (6) and (9) also plays a role. The next is more complicated: Sb atom reacts to form  $\text{SbO}_2$  (via reaction (2) or reactions (1) followed by (3)). Reactions of  $\text{SbO}_2$  with  $\text{H}_2$  and  $\text{H}_2\text{O}$  lead to the formation of antimonic acid ( $\text{HOSbO}$ ). The reaction of  $\text{HOSbO}$  with hydrogen atom (9) leads to  $\text{SbO}$  and  $\text{H}_2\text{O}$  and completes the second cycle.

For the present conditions (stoichiometric methane flame with initial  $\text{SbH}_3$  volume fraction of 0.25 %) the first cycle is about 30 % as important of the second cycle (based on the Sb-atom consumption rates). A rough estimate of the regeneration coefficient (the number of radicals recombined per molecule of active catalytic species) (Noto et al., 1998) shows that it is in the range of 15 to 25 (depending on agent concentration and conditions). This value reflects a higher inhibition effectiveness of antimony-containing compounds in comparison with  $\text{CF}_3\text{Br}$ , which has an estimated regeneration coefficient between 5 and 7 (Noto et al., 1998).

The antimony catalytic cycles of Figure 7 can be compared to those of phosphorous (e.g., DMMP (Babushok and Tsang, 1999, Jayaweera et al., 2005)). With antimony, reactions of Sb atom are important, whereas those of P are not; reactions of  $\text{HOSbO}_2$  are not important, but those of  $\text{HOPO}_2$  are, particularly for lean conditions. Also, reactions of  $\text{SbO}$  are important contributors to radical scavenging cycles, but those of  $\text{PO}$  are not. The relative ratios of  $[\text{PO}]:[\text{PO}_2]$  and  $[\text{SbO}]:[\text{SbO}_2]$  are also different: for the antimony system,  $[\text{SbO}_2] \ll [\text{SbO}]$  (by about 100 times), but for the phosphorus system, they are roughly of the same order of magnitude.

### 3.5. Antimony-bromine gas-phase synergism

The combination of antimony trioxide with a chlorinated or brominated species in polymers is empirically known to be a synergistic fire retardant mixture for polymers. Hence, it is of interest to explore if the present model shows any synergism in the gas-phase inhibition mechanism of a system with both Sb and Br present. To this end, the laminar burning velocity of a stoichiometric methane-air flame was calculated with an additive composed of varying levels of  $\text{SbH}_3$  and  $\text{HBr}$ . The total additive volume fraction was fixed at either of 0.1 % or 0.2 %, and the fraction of  $\text{SbH}_3$  in the inhibitor was varied from 100 % to 0 % (with the rest  $\text{HBr}$ ). Figure 8 shows the calculated burning velocity as a function of volume fraction of  $\text{HBr}$  in the total mix (total

inhibitor volume fraction of the blend is constant at 0.1 % or 0.2 %). (For reference, the uninhibited burning velocity is 37.5 cm/s). At  $X_{HBr} = 0$  ( $X_{SbH_3} = 0.001$  or  $0.002$ ), the decrease in burning velocity due to the additive is at a maximum value. Replacement of  $SbH_3$  by  $HBr$  leads to a lower decrease of burning velocity (i.e.,  $SbH_3$  is a more effective inhibitor than  $HBr$ ). A linear dependence of burning velocity with  $HBr$  volume fraction (dotted lines in Figure 8) indicates a lack of synergism (i.e., the total inhibition is a sum of the inhibition from each component of the blend); curves falling below the dotted line indicate synergism, with some interaction of inhibitors leading an increased effect.

From Figure 8, it can be seen that the  $SbH_3/HBr$  blend has a nearly linear dependence on fraction of  $HBr$  in the blend, with a slight synergism, that increases as the loading of the inhibitor increases (from 0.1 % to 0.2 % volume fraction). Nonetheless, the synergetic effect indicated by these calculations is small. Reaction rate analysis demonstrates that reaction rates of species containing both  $Sb$  and  $Br$  are small in comparison to the reaction rates of the main reactions of antimony and bromine inhibition cycles. For example, the flux of radical consumption through reactions of  $BrSbO$  is more than two orders of magnitude smaller than that caused by reactions of  $HOSbO$ ,  $SbO$ ,  $HBr$  or  $Br$ ; reaction fluxes for  $SbBr$  species are even smaller, by another order of magnitude. Moreover, a detailed analysis of possible additional  $Sb-Br$ -containing species and “cross-interaction” reactions did not reveal additional reactions which might have substantial contribution to the gas flame inhibition chemistry.

It is of interest that combining effective moieties (e.g.,  $Br$  and  $Sb$ ) in a single molecule actually reduces the availability of one of the moieties to participate in its own inhibition cycles. Hence, in order to show synergism, the combined species would have to have a particularly effective catalytic cycle to compensate for the loss of the cycle of one of the elements.

The above analysis for synergism is limited to the ideal case of two effective inhibitors already present in the gas phase, and explores the possibility of synergism in radical recombination cycles. Nonetheless, actual fire retarded polymers have many other physical and chemical processes in which synergistic action may be occurring. These include polymer and fire retardant decomposition rates (and timing), char formation, transport of the active species to gas phase, and interactions of the resultant flame (and its heat release) with the fuel decomposition (i.e., fuel generation) processes. While examination of these processes is beyond the scope of the present work, the availability of a validated gas-phase kinetic model for flame inhibition by antimony and

bromine can clearly help to distinguish between fire retardant mechanisms and synergistic effects for specific physical and chemical systems of interest.

As one example of the type of information that might prove to be useful, examination of the kinetics of antimony-inhibited flames has indicated that the species  $\text{Sb}_4\text{O}_6$  may play an unexpected role. In the polymer industry, antimony trioxide ( $\text{Sb}_2\text{O}_3$ ) is typically used as a fire retardant additive (as a synergist with brominated compounds). Since  $\text{Sb}_2\text{O}_3$  has a relatively high boiling point, 1425 °C (melting point, 655 °C), antimony may be transported to the gas-phase via antimony trihalides or antimony oxyhalides (resulting from reaction of  $\text{Sb}_2\text{O}_3$  with halogenated species in the condensed phase) (Hastie, 1973a, Hastie and McBee, 1975). Nonetheless,  $\text{Sb}_2\text{O}_3$  likely forms as an intermediate species in the gas phase, and experimental measurements show that  $\text{Sb}_2\text{O}_3$  then forms  $\text{Sb}_4\text{O}_6$  as a main antimony compound in the gas phase (Asryan et al., 2004, Behrens and Rosenblat, 1973, Kunkel et al., 2014). Preliminary flame equilibrium estimates (using thermochemistry of  $\text{Sb}_4\text{O}_6$  from (Gurvich et al., 1993)) demonstrate that this compound is rather stable at high temperatures, and may survive in a combustion atmosphere up to 1400 K to 1700 K. This high stability of  $\text{Sb}_4\text{O}_6$  in the gas phase should lead to the delay in formation of the species active in the catalytic cycle (Sb, SbO,  $\text{SbO}_2$  and HOSbO), and hence delay of inhibition processes. While rudimentary reactions for the formation and consumption of the species  $\text{Sb}_4\text{O}_6$  are not in the present mechanism, its formation may play an important role in the effectiveness of antimony compounds as gas-phase fire retardants. Moreover, since the condensation process is strongly influenced by the time-temperature history in the flowfield of the relevant flame (i.e., fire) (Rumminger and Linteris, 2002), any sequestration of the active Sb compounds to  $\text{Sb}_4\text{O}_6$  may be strongly affected by the particular flame structure of the test method, fire, or polymer of interest.

#### **4. Conclusions**

The present work has developed the first detailed kinetic model for gas-phase flame inhibition by antimony compounds, as well as ones for antimony/chlorine and antimony/bromine systems. These models can serve as the basis for further development, testing, and refinement. The first steps at model validation were made using available data from literature, and the model was applied via premixed flame speed simulations to gain insight into gas-phase flame inhibition by antimony/halogen compounds. The main results of the present study are:

1) Thermochemical data for the relevant species of Sb-Br-Cl-H-C-O compounds in flame environments were assembled from the literature; when needed data were missing, they were calculated. These data provide a basis for flame inhibition models by Sb-, Cl-, and Br-containing compounds.

2) Combustion equilibrium calculations were performed to determine the main antimony-bromine species in combustion products and in a flame reaction zone. Calculations were performed for species distribution as a function of combustion temperature, equivalence ratio, and inhibitor loading for representative compounds ( $\text{SbH}_3$  and  $\text{SbBr}_3$ ) in a methane/air flame.

3) Based on the equilibrium calculation results and other considerations, a limited set of species was developed for inclusion in the kinetic model for flames inhibition. These include: Sb,  $\text{SbO}$ ,  $\text{SbO}_2$ ,  $\text{SbO}_3$ ,  $\text{HOSbO}$ ,  $\text{HOSbO}_2$ ,  $\text{SbH}$ ,  $\text{SbOH}$ ,  $\text{Sb}_2$ ,  $\text{BrSbO}$ ,  $\text{SbBr}$ ,  $\text{SbBr}_2$ ,  $\text{SbBr}_3$ ,  $\text{SbH}_3$  and  $\text{SbH}_2$ . The reactions of the major species and radicals of hydrocarbon flames with these antimony/halogen-containing species were considered. The antimony/halogen sub-kinetic model was combined with Grimech-3.0 for methane-air flames, and included the bromine-species reactions from a flame inhibition model for  $\text{CF}_3\text{Br}$ .

4) To explore the model performance and relative efficiency of antimony/halogen systems, the burning velocity of methane-air flames was calculated for addition of  $\text{SbH}_3$ ,  $\text{SbBr}_3$ ,  $\text{SbCl}_3$ ,  $\text{Sb}_4\text{O}_6$ ,  $\text{BrSbO}$  and  $\text{ClSbO}$ , and the results compared to other well-studied flame inhibitors ( $\text{HBr}$ ,  $\text{CF}_3\text{Br}$  and trimethylphosphate). The results indicate that the performance of the antimony compounds is intermediate between compounds of bromine and phosphorus compounds (e.g.,  $\text{CF}_3\text{Br}$ , TMP). As was expected,  $\text{SbBr}_3$  is more effective than  $\text{SbCl}_3$  and  $\text{SbH}_3$ , and  $\text{BrSbO}$  is more effective than  $\text{ClSbO}$ .

5) For the antimony-inhibited premixed flames, reaction pathway analysis revealed the radical scavenging sequences. The catalytic radical recombination sequences include the species: Sb,  $\text{SbO}$ ,  $\text{SbO}_2$  and  $\text{HOSbO}$  (in contrast to the phosphorus catalytic cycles that are dominated by  $\text{HOPO}$ ,  $\text{HOPO}_2$ ,  $\text{PO}_2$  and  $\text{PO}$ ).

6) Analysis of methane-air flame inhibition by a model Sb/Br combination ( $\text{SbH}_3$ - $\text{HBr}$ ) did not show synergism in the gas phase; i.e., the inhibition chemistry of the Sb and Br cycles were relatively independent.

**Acknowledgements:** The author (VB) was supported by BASF.

\*Official contribution of NIST, not subject to copyright in the United States. Certain commercial equipment, instruments, and materials are identified in this paper to adequately specify procedure. Such identification does not imply recommendation or endorsement by the National Institute of Standards and Technology.

## 5. References

- Ahlich, R., Bar, M., Haser, M., Horn, H. & Kolmel, C. 1989. Electronic-structure calculations on workstation computers - the program system turbomole. *Chem. Phys. Lett.*, 162, 165-169.
- Andrews, G. E. & Bradley, D. 1972. Determination of burning velocities: a critical review. *Combust. Flame*, 18, 133-153.
- Asryan, N. A., Alikhanyan, A. S. & Nipan, G. D. 2004. P-T-x phase diagram of the Sb-O system. *Inorg. Mater.*, 40, 626-631.
- Babushok, V. & Tsang, W. 2000. Inhibitor rankings for alkane combustion. *Combust. Flame*, 123, 488-506.
- Babushok, V. I., Linteris, G. T., Burgess, D. R. & Baker, P. T. 2015. Hydrocarbon flame inhibition by C<sub>3</sub>H<sub>2</sub>F<sub>3</sub>Br (2-BTP). *Combust. Flame*, 162, 1104-1112.
- BABUSHOK, V. I., LINTERIS, G. T. & MEIER, O. C. 2012. Combustion properties of halogenated fire suppressants. *Combust. Flame*, 159, 3569-3575.
- Babushok, V. I., Linteris, G. T., Meier, O. C. & Pagliaro, J. L. 2014. Flame inhibition by CF<sub>3</sub>CHCL<sub>2</sub> (HCFC-123). *Combust. Sci. Technol.*, 186, 792-814.
- Babushok, V. I. & Tsang, W. Influence of phosphorus-containing fire suppressants on flame propagation. International Conference on Fire Research and Engineering (ICFRE3), 1999 Chicago, IL. Boston, MA: Society of Fire Protection Engineers (SFPE), 257-267.
- Behrens, R. G. & Rosenblat, G.M. 1973. Vapor-pressure and thermodynamics of orthorhombic antimony trioxide (valentinite). *J. Chem. Thermodyn.*, 5, 173-188.
- Burcat, A., Olchanski, E. & Sokolinski, C. 1996. Kinetics of hexane combustion in a shock tube. *Israel J. Chem.*, 36, 313-320.
- Dixon-lewis, G. & Simpson, R. J. 1977. Aspects of flame inhibition by halogen compounds. *Proc. Combust. Inst.*, 16, 1111-1119.
- Farber, M. & Srivastava, R. D. 1975. Investigation of arsenic and antimony additives in unseeded and potassium-seeded H<sub>2</sub>-O<sub>2</sub> flames. *Combust. Flame*, 25, 101-106.

- Fenimore, C. & Jones, G. W. 1966. Modes of inhibiting polymer flammability. *Combust. Flame*, 10, 295-301.
- Fenimore, C. P. & Martin, F. J. 1966a. Candle-type test for flammability of polymers. *Modern Plastics*, 12, 141-192.
- Fenimore, C. P. & Martin, F. J. 1966b. Flammability of polymers. *Combust. Flame*, 10, 135-139.
- Fenimore, C. P. & Martin, F. J. 1972. Burning of polymers. In: WALL, L. A. (ed.) *The mechanisms of pyrolysis, oxidation and burning of organic materials*. Washington, D.C.: National Bureau of Standards.
- Goos, E., Burcat, A. & Ruscic, B. 2012. *Extended Third Millennium Thermodynamic Database for Combustion and Air-Pollution Use with updates from Active Thermochemical Tables* [Online]. Aerospace Engineering, Technion-IIT Haifa Israel. Available: <ftp://ftp.technion.ac.il/pub/supported/aetdd/thermodynamics/BURCAT.THR> [Accessed August 2012].
- Gurvich, L. V., Iorish, V. S., Chekhovskoi, D. V., Ivanisov, A. D., Proskurnev, A. Y., Yungman, V. S., Medvedev, V. A., Veits, I. V. & Bergman, G. A. 1993. *IVTHANTHERMO. Database on Thermodynamic Properties of Individual Substances.*, Moscow (NIST Special Database 5, IVTANTHERMO-PC, 1998), Institute of High Temperatures.
- Hastie, J. W. 1973a. Mass-spectrometric studies of flame inhibition - analysis of antimony trihalides in flames. *Combust.Flame*, 21, 49-54.
- Hastie, J. W. 1973b. Molecular basis of flame inhibition. *J. Res. Nat. Bureau of Standards Section a-Phys. Chem.*, A 77, 733-754.
- Hastie, J. W., Bonnell, D. W. & Schenck, P. K. 1986. Molecular Basis for Secondary Flash Suppression. Report, MIPR 102-84, National Bureau of Standards, 23 p.
- Hastie, J. W. & McBee, C. L. 1975. Mechanistic studies of halogenated flame retardants - antimony-halogen system. *ACS Symp. Ser.*, 16,118-148.
- Jayaweera, T. M., Melius, C. F., Pitz, W. J., Westbrook, C. K., Korobeinichev, O. P., Shvartsberg, V. M., Shmakov, A. G., Rybitskaya, I. V. & Curran, H. J. 2005. Flame inhibition by phosphorus-containing compounds over a range of equivalence ratios. *Combust. Flame*, 140, 103-115.
- Khalturinskii, N. A. & Rudakova, T. A. 2008. Physical aspects of polymer combustion and the inhibition mechanism. *Rus. J. Phys. Chem. B*, 2, 480-490.
- Kunkel, K., Milke, E. & Binnewies, M. 2014. A mass spectrometric and quantum chemical study of the vaporisation of lead monoxide in a flow of gaseous arsenic and antimony trioxides. *Dalton Trans.*, 43, 5401-5408.

- Lask, G. & Wagner, H. G. 1962. Influence of additives on the velocity of laminar flames. *Proc. Combust. Inst.*, 8, 432-438.
- Lewin, M. 1999. Synergistic and catalytic effects in flame retardancy of polymeric materials - An overview. *J. Fire Sci.*, 17, 3-19.
- Lewin, M. 2001. Synergism and catalysis in flame retardancy of polymers. *Polym Adv. Technol.*, 12, 215-222.
- Linteris, G. T. 2002. Gas-Phase Mechanisms of Fire Retardants. Report, NISTIR 6889, Gaithersburg, MD, NIST.
- Linteris, G. T., Knyazev, V. D. & Babushok, V. I. 2002. Inhibition of premixed methane flames by manganese and tin compounds. *Combust. Flame*, 129, 221-238.
- Linteris, G. T., Rumminger, M. D., Babushok, V. I. & Tsang, W. 2000. Flame inhibition by ferrocene and blends of inert and catalytic agents. *Proc. Combust. Inst.*, 28, 2965-2972.
- McHale, E. T. 1969. Survey of vapor phase chemical agents for combustion suppression. *Fire Research Abstracts and Reviews*, 11, 90-104.
- Miller, D. R., Evers, R. L. & Skinner, G. B. 1963. Effects of various inhibitors on hydrogen air flame speeds. *Combust. Flame*, 7, 137-142.
- Noto, T., Babushok, V., Hamins, A. & Tsang, W. 1998. Inhibition effectiveness of halogenated compounds. *Combust. Flame*, 112, 147-160.
- Reynolds, W. C. 1986. The element potential method for chemical equilibrium analysis: implementation in the interactive program STANJAN. Version 3 ed. Stanford, CA: Stanford University.
- Rumminger, M. D. & Linteris, G. T. 2002. The role of particles in the inhibition of counterflow diffusion flames by iron pentacarbonyl. *Combust. Flame*, 128, 145-164.
- Salmeia, K. A., Fage, J., Liang, S. Y. & Gaan, S. 2015. An overview of mode of action and analytical methods for evaluation of gas phase activities of flame retardants. *Polymers*, 7, 504-526.
- Skulan, A. J., Nielsen, I. M. B., Melius, C. F. & Allendorf, M. D. 2006. BAC-MP4 predictions of thermochemistry for gas-phase antimony compounds in the Sb-H-C-O-Cl system. *J. Phys. Chem. A*, 110, 5919-5928.
- Smith, G. P., Golden, D. M., Frenklach, M., Moriarty, N. W., Eiteneer, B., Goldenberg, M., Bowman, C. T., Hanson, R. K., Song, S., Gardiner, J. W. C., Lissianski, V. V. & Qin, Z. 2000. *GRI Mech 3.0* [Online]. Berkeley, CA: University of California, Berkeley. Available: [http://www.me.berkeley.edu/gri\\_mech](http://www.me.berkeley.edu/gri_mech) [Accessed Sept. 9, 2015 2015].
- Wang, H., You, X., Jucks, K. W., Davis, S. G., Laskin, A., Egolfopoulos, F. & Law, C. K. 2007. *USC Mech Version II. High-temperature combustion reaction model of H2/CO/Cl-C4*



*compounds* [Online]. Los Angeles, CA: University of Southern California. Available: [http://ignis.usc.edu/USC\\_Mech\\_II.htm](http://ignis.usc.edu/USC_Mech_II.htm) [Accessed 2015 2015].

Weil, E. D. 2011. Fire-protective and flame-retardant coatings - A state-of-the-art review. *J. Fire Sci.*, 29, 259-296.

Weil, E. D. & Levchik, S. V. 2007. Flame retardants for polystyrenes in commercial use or development. *J. Fire Sci.*, 25, 241-265.

Westbrook, C. K. 1982. Inhibition of hydrocarbon oxidation in laminar flames and detonations by halogenated compounds. *Proc. Symp. Combust.*, 19, 127-141.

Table 1 - Thermodynamic data of antimony-containing species (1 bar).

Species	Reaction used for calculations	$\Delta H_f$ [kJ/mol]	S [J/mol/K]	$C_p$ [J/mol/K]	Reference
Sb		264.6	180.3	20.79	(Goos et al., 2012)
Sb <sub>2</sub>		236	255.9	36.41	(Goos et al., 2012)
SbH		246.4	215.9	29.2	(Skulan et al., 2006)
SbH <sub>2</sub>		207.4	234.3	35.92	(Goos et al., 2012)
SbH <sub>3</sub>		144.8	232.7	41.22	(Goos et al., 2012)
SbCl		94.5	257.3	35.93	(Skulan et al., 2006)
SbCl <sub>2</sub>		-98.7	280.8	43.23	(Goos et al., 2012)
SbCl <sub>3</sub>		-313.4	341.1	77.39	(Goos et al., 2012)
SbCl <sub>4</sub>		-290.8	407.8	94.26	(Skulan et al., 2006), est
SbCl <sub>5</sub>		-433.0	422.2	122.1	(Goos et al., 2012)
ClSbO		-106.7	299.8	50.83	(Hastie and McBee, 1975), est
SbO	$SbH_3 + 1.25O_2 = SbO + 1.5 H_2O$	+137.6	244.4	32.01	This work
HSbO	$SbH_3 + O_2 = HSbO + H_2O$	+90.2	267.8	40.11	This work
Sb(OH)	$SbH_3 + O_2 = Sb(OH) + H_2O$	+43.7	264.4	40.54	This work
HOSbH		-15.5	278.1	50.77	(Skulan et al., 2006)
OSbH <sub>2</sub>		185.8	272.7	49.51	(Skulan et al., 2006)
HOSbH <sub>2</sub>		-75.7	274.6	58.56	(Skulan et al., 2006)
SbO <sub>2</sub>	$SbH_3 + 1.75O_2 = SbO_2 + 1.5 H_2O$	+29.3	293.4	48.52	This work
HSbO <sub>2</sub>	$SbH_3 + 1.5 O_2 = HSbO_2 + H_2O$	+18.7	302.4	57.83	This work
(HO)SbO	$SbH_3 + 1.5 O_2 = (HO)SbO + H_2O$	-233.8	302.6	56.24	This work
(HO)HSbO	$SbH_3 + 1.25 O_2 = (HO)HSbO + 0.5 H_2O$	-112.3	313.5	69.88	This work
Sb(OH) <sub>2</sub>	$SbH_3 + 1.25 O_2 = Sb(OH)_2 + 0.5 H_2O$	-283.8	325.1	70.74	This work
(HO) <sub>2</sub> SbH		-339.3	308.9	75.69	(Skulan et al., 2006)
SbO <sub>3</sub>	$SbH_3 + 2.25O_2 = SbO_3 + 1.5 H_2O$	+99.0	336.6	69.39	This work

(HO)SbO <sub>2</sub>	SbH <sub>3</sub> + 2 O <sub>2</sub> = (HO)SbO <sub>2</sub> + H <sub>2</sub> O	-252.7	336.9	75.21	This work
(HO) <sub>2</sub> HSbO	SbH <sub>3</sub> + 1.5 O <sub>2</sub> = (HO) <sub>2</sub> HSbO	-458.8	348.6	95.22	This work
Sb(OH) <sub>3</sub>	SbH <sub>3</sub> + 1.5 O <sub>2</sub> = Sb(OH) <sub>3</sub>	-664.0	347.2	98.49	This work
(HO) <sub>2</sub> SbO <sub>2</sub>	SbH <sub>3</sub> + 2.25 O <sub>2</sub> = (HO) <sub>2</sub> SbO <sub>2</sub> + 0.5 H <sub>2</sub> O	-418.8	388.9	108.62	This work
(HO) <sub>3</sub> SbO	SbH <sub>3</sub> + 2 O <sub>2</sub> = (HO) <sub>3</sub> SbO	-718.4	386.3	116.12	This work
SbBr	SbH <sub>3</sub> + HBr + O <sub>2</sub> = SbBr + 2 H <sub>2</sub> O	+185.8	268.6	36.51	This work
HSbBr	SbH <sub>3</sub> + HBr + 0.75 O <sub>2</sub> = HSbBr + 1.5 H <sub>2</sub> O	+131.9	292.5	45.29	This work
H <sub>2</sub> SbBr	SbH <sub>3</sub> + HBr + 0.5 O <sub>2</sub> = H <sub>2</sub> SbBr + H <sub>2</sub> O	+60.3	296.1	52.58	This work
BrSbO	SbH <sub>3</sub> + HBr + 1.5 O <sub>2</sub> = BrSbO + 2 H <sub>2</sub> O	-54.9	322.8	51.42	This work
(HO)SbBr	SbH <sub>3</sub> + HBr + 1.25 O <sub>2</sub> = (HO)SbBr + 1.5 H <sub>2</sub> O	-129.4	334.5	63.56	This work
BrSbO <sub>2</sub>	SbH <sub>3</sub> + HBr + 2 O <sub>2</sub> = BrSbO <sub>2</sub> + 2 H <sub>2</sub> O	-73.4	350.9	70.19	This work
(HO)BrSbO	SbH <sub>3</sub> + HBr + 1.75 O <sub>2</sub> = (HO)BrSbO + 1.5 H <sub>2</sub> O	-213.3	370.7	83.62	This work
(HO) <sub>2</sub> SbBr	SbH <sub>3</sub> + HBr + 1.5 O <sub>2</sub> = (HO) <sub>2</sub> SbBr + H <sub>2</sub> O	-495.0	372.9	92.60	This work
(HO) <sub>2</sub> BrSbO	SbH <sub>3</sub> + HBr + 2 O <sub>2</sub> = (HO) <sub>2</sub> BrSbO + H <sub>2</sub> O	-536.7	408.0	111.29	This work
SbBr <sub>2</sub>	SbH <sub>3</sub> + 2 HBr + 1.25 O <sub>2</sub> = SbBr <sub>2</sub> + 2.5 H <sub>2</sub> O	+29.8	341.6	56.39	This work
HSbBr <sub>2</sub>	SbH <sub>3</sub> + 2 HBr + O <sub>2</sub> = HSbBr <sub>2</sub> + 2 H <sub>2</sub> O	-35.0	349.7	65.64	This work
Br <sub>2</sub> SbO	SbH <sub>3</sub> + 2 HBr + 1.75 O <sub>2</sub> = Br <sub>2</sub> SbO + 2.5 H <sub>2</sub> O	-44.0	383.2	76.75	This work
(HO)SbBr <sub>2</sub>	SbH <sub>3</sub> + 2 HBr + 1.5 O <sub>2</sub> = (HO)SbBr <sub>2</sub> + 2 H <sub>2</sub> O	-320.4	387.7	86.79	This work
SbBr <sub>3</sub>	SbH <sub>3</sub> + 3 HBr + 1.5 O <sub>2</sub> = SbBr <sub>3</sub> + 3 H <sub>2</sub> O	-139.9	393.4	80.33	This work
Br <sub>3</sub> SbO	SbH <sub>3</sub> + 3 HBr + 2 O <sub>2</sub> = Br <sub>3</sub> SbO + 3 H <sub>2</sub> O	-175.8	422.4	98.89	This work
CH <sub>3</sub> SbO <sub>2</sub>	SbH <sub>3</sub> + CH <sub>4</sub> + 2 O <sub>2</sub> = CH <sub>3</sub> SbO <sub>2</sub> + 2 H <sub>2</sub> O	-51.8	363.2	84.12	This work
(CH <sub>3</sub> O)SbO	SbH <sub>3</sub> + CH <sub>4</sub> + 2 O <sub>2</sub> = (CH <sub>3</sub> O)SbO + 2 H <sub>2</sub> O	-202.0	342.9	76.68	This work
(CH <sub>3</sub> O)SbO <sub>2</sub>	SbH <sub>3</sub> + CH <sub>4</sub> + 2.5 O <sub>2</sub> = (CH <sub>3</sub> O)SbO <sub>2</sub> + 2 H <sub>2</sub> O	-219.8	348.1	96.03	This work
CH <sub>3</sub> SbBr	SbH <sub>3</sub> +CH <sub>4</sub> +HBr+1.25O <sub>2</sub> = CH <sub>3</sub> SbBr + 2.5 H <sub>2</sub> O	+82.0	342.7	70.78	This work
CH <sub>3</sub> SbBr <sub>2</sub>	SbH <sub>3</sub> +CH <sub>4</sub> +2HBr+1.5O <sub>2</sub> = CH <sub>3</sub> SbBr <sub>2</sub> + 3 H <sub>2</sub> O	-100.6	395.1	94.00	This work
(HO)(CH <sub>3</sub> )SbBr	SbH <sub>3</sub> +CH <sub>4</sub> +HBr+1.5O <sub>2</sub> =(HO)CH <sub>3</sub> SbBr+2H <sub>2</sub> O	-264.5	380.1	99.49	This work
(CH <sub>3</sub> ) <sub>2</sub> SbBr	SbH <sub>3</sub> +2CH <sub>4</sub> +HBr+1.5O <sub>2</sub> =(CH <sub>3</sub> ) <sub>2</sub> SbBr+3H <sub>2</sub> O	-48.0	388.8	107.63	This work
Sb(CH <sub>3</sub> )		217.1	273.5	46.81	(Skulan et al., 2006)
Sb(CH <sub>3</sub> ) <sub>2</sub>		143.93	326.2	78.06	(Goos et al., 2012)
Sb(CH <sub>3</sub> ) <sub>3</sub>		38.5	361.1	111.0	(Goos et al., 2012)
SbH(CH <sub>3</sub> )		177.8	286.4	55.86	(Skulan et al., 2006)
SbH <sub>2</sub> CH <sub>3</sub>		114.2	285.9	63.12	(Skulan et al., 2006)
SbH(CH <sub>3</sub> ) <sub>2</sub>		78.7	329.2	86.85	(Skulan et al., 2006)
Sb(CH <sub>3</sub> )(OH)		-59.8	324.1	72.32	(Skulan et al., 2006)
SB(CH <sub>3</sub> ) <sub>2</sub> (OH)		-169.5	366.4	107.38	(Skulan et al., 2006)
SB(CH <sub>3</sub> )(OH) <sub>2</sub>		-394.1	353.2	103.19	(Skulan et al., 2006)

$\text{SB(H)}_2\text{CH}_2$		323.4	294.6	63.61	(Skulan et al., 2006)
$\text{Sb}_4\text{O}_6$		-1222.3	462.3	188.84	(Gurvich et al., 1993)

**Table 2 - Kinetic model for antimony/bromine containing species (units: mole,s,cm,kJ).**

No	Reaction	A	n	E
1.	H+SBO=SB+OH	2.70E+13	0	31.38
2.	SBO+OH+M=HOSBO+M H2O/16/ H2/2.5/	4.00E+22	-2.1	6.65
3.	SBO+O+M=SBO2+M H2O/16/ H2/2.5/	4.80E+25	-2.6	7.20
4.	CH3+SBO2=CH3O+SBO	2.00E+13	0	41.84
5.	SBO+HO2=SBO2+OH	2.00E+12	0	29.29
6.	SBO+O=SB+O2	7.20E+09	1	12.55
7.	H+SBO2+M=HOSBO+M H2O/16/ H2/2.5/	4.87E+23	-2	2.70
8.	SBO2+OH+M=HOSBO2+M H2O/16/ H2/2.5/	1.60E+24	-2.3	1.19
9.	SBO2+O+M=SBO3+M H2O/16/ H2/2.5/	1.30E+27	-3.1	7.87
10.	SBO2+HCO=HOSBO+CO	1.20E+23	-3.3	9.79
11.	SBO2+HCO=CO2+SBO+H	8.40E+15	-0.8	8.08
12.	SBO2+CH2O=HCO+HOSBO	2.00E+12	0	23.01
13.	SBO2+CH4=HOSBO+CH3	3.00E+12	0	37.66
14.	SBO2+C2H6=HOSBO+C2H5	2.50E+12	0	33.47
15.	SBO2+H2O2=HO2+HOSBO	2.50E+12	0	31.38
16.	SBO2+H=OH+SBO	4.30E+13	0	29.29
17.	SBO2+O=SBO+O2	2.50E+13	0	8.37
18.	SBO3+H=SBO2+OH	6.60E+13	0	0.00
19.	SBO+SBO3=SBO2+SBO2	1.10E+13	0	4.18
20.	SBO2+HO2=O2+HOSBO	2.40E+13	0	0.00
21.	SBO3+CH3=SBO2+CH3O	2.00E+13	0	6.28
22.	SBO2+CH3O=CH2O+HOSBO	3.00E+13	0	0.00
23.	SBO2+CH3OH=HOSBO+CH3O	3.00E+12	0	37.66
24.	SBO2+CH3OH=HOSBO+CH2OH	8.00E+12	0	33.47
25.	SBO2+OH=HOSBO+O	2.40E+13	0	37.66
26.	SBO3+H+M=HOSBO2+M H2O/16/ H2/2.5/	4.80E+24	-2.4	5.98
27.	SBO3+HCO=HOSBO2+CO	3.50E+13	0	0.00
28.	SBO3+CH3O=HOSBO2+CH2O	1.80E+13	0	0.00
29.	SBO3+H2O2=HO2+HOSBO2	1.50E+12	0	14.64
30.	SBO3+OH=HOSBO2+O	6.00E+12	0	20.92
31.	SBO3+OH=HO2+SBO2	1.10E+13	0	23.01
32.	SBO3+CH2O=HOSBO2+HCO	2.50E+12	0	6.28
33.	SBO3+CH4=CH3+HOSBO2	2.00E+12	0	18.83
34.	SBO3+C2H6=C2H5+HOSBO2	3.00E+12	0	13.39
35.	SBO3+H=HOSBO+O	2.00E+12	0	4.18

36.	$\text{SBO}_3 + \text{H}_2 = \text{HOSBO}_2 + \text{H}$	$1.40\text{E}+12$	0	23.85
37.	$\text{SBO}_3 + \text{HOSBO} = \text{SBO}_2 + \text{HOSBO}_2$	$2.50\text{E}+12$	0	18.41
38.	$\text{SBO}_3 + \text{O} = \text{SBO}_2 + \text{O}_2$	$1.80\text{E}+13$	0	0.00
39.	$\text{HOSBO} + \text{O} + \text{M} = \text{HOSBO}_2 + \text{M}$ H2O/16/ H2/2.5/	$2.40\text{E}+27$	-3	8.54
40.	$\text{HOSBO} + \text{H} = \text{H}_2 + \text{SBO}_2$	$2.00\text{E}+13$	0	81.59
41.	$\text{HOSBO} + \text{H} = \text{H}_2\text{O} + \text{SBO}$	$3.20\text{E}+13$	0	30.96
42.	$\text{HOSBO} + \text{OH} = \text{SBO}_2 + \text{H}_2\text{O}$	$2.40\text{E}+06$	2	43.93
43.	$\text{HOSBO} + \text{O} = \text{O}_2 + \text{SBOH}$	$6.50\text{E}+12$	0	62.76
44.	$\text{HOSBO}_2 + \text{H} = \text{H}_2\text{O} + \text{SBO}_2$	$1.80\text{E}+13$	0	8.37
45.	$\text{HOSBO}_2 + \text{H} = \text{HOSBO} + \text{OH}$	$3.80\text{E}+05$	2.3	10.46
46.	$\text{HOSBO}_2 + \text{O} = \text{HOSBO} + \text{O}_2$	$1.60\text{E}+13$	0	0.00
47.	$\text{HOSBO}_2 + \text{OH} = \text{H}_2\text{O} + \text{SBO}_3$	$2.40\text{E}+06$	2	96.23
48.	$\text{HOSBO}_2 + \text{OH} = \text{HOSBO} + \text{HO}_2$	$6.00\text{E}+12$	0	43.93
49.	$\text{HOSBO}_2 + \text{O}_2 = \text{HO}_2 + \text{SBO}_3$	$7.00\text{E}+12$	0	276.14
50.	$\text{HOSBO}_2 + \text{CH}_3 = \text{CH}_3\text{O} + \text{HOSBO}$	$3.00\text{E}+12$	0	33.47
51.	$\text{HOSBO}_2 + \text{CH}_2 = \text{CH}_2\text{O} + \text{HOSBO}$	$4.00\text{E}+10$	0	0.00
*52.	$\text{SB} + \text{O}_2 + \text{M} = \text{SBO}_2 + \text{M}$ H2O/16/ H2/2.5/	$1.16\text{E}+17$	0	0.00
53.	$\text{SB} + \text{O} + \text{M} = \text{SBO} + \text{M}$ H2O/16/ H2/2.5/	$3.30\text{E}+17$	0	0.00
54.	$\text{SB} + \text{SBO}_3 = \text{SBO} + \text{SBO}_2$	$2.00\text{E}+13$	0	0.00
55.	$\text{SB} + \text{SBO}_2 = \text{SBO} + \text{SBO}$	$7.00\text{E}+12$	0	43.93
56.	$\text{SB} + \text{CH}_3\text{O} = \text{SBO} + \text{CH}_3$	$2.50\text{E}+13$	0	50.21
57.	$\text{SB} + \text{HOSBO}_2 = \text{SBO} + \text{HOSBO}$	$1.50\text{E}+12$	0	18.83
58.	$\text{SBH}_3 = \text{SBH}_2 + \text{H}$	$6.60\text{E}+17$	0	288.70
59.	$\text{SBH}_2 = \text{SBH} + \text{H}$	$2.00\text{E}+16$	0	263.59
60.	$\text{SBH}_3 + \text{H} = \text{SBH}_2 + \text{H}_2$	$4.40\text{E}+13$	0	10.46
61.	$\text{SBH}_3 + \text{O} = \text{SBH}_2 + \text{OH}$	$2.80\text{E}+13$	0	10.46
62.	$\text{SBH}_3 + \text{OH} = \text{SBH}_2 + \text{H}_2\text{O}$	$1.60\text{E}+13$	0	0.00
63.	$\text{SBH}_3 + \text{CH}_3 = \text{SBH}_2 + \text{CH}_4$	$4.00\text{E}+11$	0	12.55
64.	$\text{SBH}_3 + \text{HCO} = \text{SBH}_2 + \text{CH}_2\text{O}$	$6.00\text{E}+11$	0	25.10
65.	$\text{SBH}_2 + \text{H} = \text{SBH} + \text{H}_2$	$6.30\text{E}+13$	0	4.18
66.	$\text{SBH}_2 + \text{O} = \text{SBH} + \text{OH}$	$7.00\text{E}+12$	0	6.28
67.	$\text{SBH}_2 + \text{O} = \text{SBOH} + \text{H}$	$1.40\text{E}+13$	0	4.18
68.	$\text{SBH}_2 + \text{OH} = \text{SBH} + \text{H}_2\text{O}$	$3.20\text{E}+11$	0	0.00
69.	$\text{SBH}_2 + \text{HCO} = \text{SBH}_3 + \text{CO}$	$8.50\text{E}+12$	0	0.00
70.	$\text{SBH}_2 + \text{CH}_3 = \text{SBH} + \text{CH}_4$	$1.50\text{E}+13$	0	6.28
71.	$\text{SBH}_2 + \text{HCO} = \text{SBH} + \text{CH}_2\text{O}$	$6.00\text{E}+11$	0	20.92
72.	$\text{SBH}_2 + \text{SBH}_2 = \text{SBH}_3 + \text{SBH}$	$3.00\text{E}+11$	0	43.93
73.	$\text{SBH}_2 + \text{SB} = \text{SBH} + \text{SBH}$	$1.50\text{E}+12$	0	62.76
74.	$\text{SB} + \text{H} + \text{M} = \text{SBH} + \text{M}$	$2.00\text{E}+16$	0	0.00
75.	$\text{SBH} + \text{CH}_3 = \text{CH}_4 + \text{SB}$	$6.70\text{E}+13$	0	0.00
76.	$\text{SB} + \text{HCO} = \text{SBH} + \text{CO}$	$8.00\text{E}+13$	0	4.18

77. SBH+O=SB+OH	3.00E+13	0	0.00
78. SBH+H=SB+H2	5.00E+13	0	0.00
79. SBH+OH=SB+H2O	2.00E+13	0	0.00
80. SB+CH3O=SBH+CH2O	2.00E+13	0	8.37
81. SBH+HCO=SB+CH2O	1.00E+13	0	14.64
82. SB+HO2=SBH+O2	2.00E+13	0	41.84
83. SBH+SBO2=SB+HOSBO	3.50E+12	0	0.00
84. SBH+SBO3=SB+HOSBO2	4.00E+12	0	0.00
85. SBH+SBH2=SBH3+SB	6.50E+11	0	39.75
86. SB+SB+M=SB2+M	4.00E+16	0	0.00
87. SB2+O=SBO+SB	1.00E+13	0	25.10
88. SB2+O2=SBO+SBO	7.50E+12	0	83.68
89. SB+SBH=SB2+H	9.00E+12	0	33.47
90. SBO+SBH=SB2+OH	6.50E+12	0	20.92
91. SBH+SBO2=SB2+HO2	3.00E+12	0	39.75
92. SB+SBO2=SB2+O2	2.00E+12	0	36.40
93. SBO+SBH=SBOH+SB	6.00E+12	0	35.98
94. SB+OH+M=SBOH+M	4.00E+16	0	0.00
95. SBO+HCO=SBOH+CO	3.00E+13	0	0.00
96. SBOH+H=SBO+H2	1.00E+13	0	16.74
97. SBOH+H=SB+H2O	2.00E+12	0	6.28
98. SBOH+OH=SBO+H2O	7.30E+12	0	4.18
99. SBOH+O=SBO+OH	1.50E+13	0	20.92
100. SBOH+CH3=CH4+SBO	1.20E+13	0	18.83
101. SBOH+HO2=SBO+H2O2	1.00E+13	0	43.10
102. SBOH+CH3O=SBO+CH3OH	2.00E+12	0	18.41
Sb-Br subset			
103. BRSBO+H=HBR+SBO	3.50E+13	0	31.38
104. BRSBO+H=SBBR+OH	3.00E+13	0	87.86
105. BRSBO+OH=BR+HOSBO	6.00E+12	0	25.10
106. BRSBO+OH=BROH+SBO	1.00E+13	0	96.23
107. BRSBO+O=BR+SBO2	6.00E+12	0	33.47
108. BRSBO+O=SBBR+O2	2.00E+13	0	46.02
109. BRSBO+O=BRO+SBO	1.00E+13	0	100.42
110. SBO+BR+M=BRSBO+M	2.00E+16	0	0.00
111. SBBR+O+M=BRSBO+M	4.00E+16	0	0.00
112. SBBR+SBO=BRSBO+SB	2.00E+12	0	27.20
113. SBBR+SBO2=BRSBO+SBO	4.00E+12	0	18.83
114. SBBR+SBO3=BRSBO+SBO2	1.00E+13	0	2.09
115. SBO+BR2=BRSBO+BR	3.00E+13	0	20.92
116. BROH+SBBR=HBR+BRSBO	1.50E+11	0	10.46
117. BRSBO+BROH=BR2+HOSBO	7.00E+11	0	33.47
118. SBO+CH3BR=BRSBO+CH3	5.00E+12	0	46.02
119. CH3BR+SBO2=CH3O+BRSBO	4.00E+12	0	46.02

120.	SBBR2+BR=SBBR3	2.00E+13	0	0.00
121.	SBBR+BR=SBBR2	2.50E+13	0	0.00
122.	SBBR3+H=SBBR2+HBR	1.02E+13	0	27.20
123.	SBBR3+OH=SBBR2+BROH	4.00E+13	0	83.68
124.	SBBR3+O=SBBR2+BRO	2.20E+13	0	75.31
125.	SBBR3+CH3=SBBR2+CH3BR	2.00E+13	0	41.84
126.	SBBR3+C2H5=C2H5BR+SBBR2	1.00E+13	0	41.84
127.	SBBR3+SBO=BRSBO+SBBR2	8.00E+12	0	39.75
128.	SBBR2+H=HBR+SBBR	1.50E+13	0	41.84
129.	SBBR2+O=SBBR+BRO	2.00E+13	0	71.13
130.	SBBR2+O=BRSBO+BR	3.50E+12	0	4.18
131.	SBBR2+OH=SBBR+BROH	2.00E+13	0	77.40
132.	SBBR2+OH=BRSBO+HBR	2.70E+12	0	8.37
133.	SBBR2+BR2=SBBR3+BR	3.30E+12	0	35.56
134.	SBBR2+BR=SBBR+BR2	1.50E+13	0	79.50
135.	SBBR2+CH3O=BRSBO+CH3BR	4.50E+11	0	16.74
136.	SBBR2+BRO=BRSBO+BR2	3.00E+11	0	6.28
137.	SBBR+SBBR=SB+SBBR2	5.00E+12	0	33.47
138.	SBBR2+SBBR2=SBBR+SBBR3	4.00E+12	0	46.02
139.	SBBR2+SBO=SBBR+BRSBO	9.00E+12	0	39.75
140.	SBBR2+SBO2=BRSBO+BRSBO	3.10E+12	0	8.37
141.	SBBR+H=HBR+SB	2.00E+13	0	4.18
142.	SBBR+O=SBO+BR	1.00E+13	0	4.18
143.	SBBR+O=SB+BRO	2.00E+13	0	41.84
144.	SBBR+OH=HBR+SBO	2.50E+12	0	20.92
145.	SBBR+OH=BROH+SB	5.00E+12	0	37.66
146.	SBBR+CH3=CH3BR+SB	8.00E+12	0	25.10
147.	SBBR+CH3O=CH3+BRSBO	1.00E+13	0	27.20
148.	SBBR+HOSBO2=BRSBO+HOSBO	2.50E+12	0	8.37
149.	SBBR+BR=SB+BR2	2.00E+13	0	41.84
150.	SBBR+BRO=BRSBO+BR	1.00E+13	0	0.00
151.	SB+BR+M=SBBR+M	2.00E+15	0	0.00
152.	BRO+SBO=BR+SBO2	1.00E+13	0	18.83
153.	SBBR+O2=BR+SBO2	2.00E+12	0	41.84
154.	BR+SBO3=BRO+SBO2	1.50E+13	0	33.47
155.	SBO2+HBR=BR+HOSBO	2.00E+11	0	17.99
156.	SBO3+HBR=BR+HOSBO2	2.00E+12	0	6.28
157.	BRO+HOSBO=BR+HOSBO2	1.00E+12	0	41.84
158.	HBR+SBO2=BRSBO+OH	1.50E+12	0	50.21
159.	BR+SBO3=BRSBO+O2	2.30E+12	0	12.55
160.	CH2+SBBR=CH2BR+SB	2.00E+13	0	14.64
161.	CH2BR+SBO=CH2O+SBBR	2.00E+12	0	0.00
162.	CH2+BRSBO=CH2BR+SBO	3.00E+13	0	43.93
163.	CH2BR+SBO2=CH2O+BRSBO	6.00E+12	0	8.37



164. BRO+SB=SBO+BR	4.00E+13	0	16.74
165. HBR+SBO3=BRO+HOSBO	8.00E+11	0	12.55
166. BROH+SBO2=BRO+HOSBO	2.00E+13	0	37.66
167. BROH+SBO3=BRO+HOSBO2	1.50E+13	0	16.74
168. BROH+SB=HBR+SBO	7.50E+11	0	29.29
169. BROH+SBO=HBR+SBO2	5.00E+11	0	33.47
170. SBBR+SB=SB2+BR	2.00E+13	0	25.10
171. SBBR+SBBR=BR2+SB2	8.00E+11	0	32.64
172. BRO+SB2=SBO+SBBR	2.00E+12	0	41.84
173. SBH+SBBR=SB2+HBR	1.00E+12	0	10.46
174. SBH+BR=HBR+SB	1.50E+13	0	18.83
175. SBH+BR2=SBBR+HBR	2.00E+12	0	20.92
176. SBH+CH2BR=SB+CH3BR	9.00E+12	0	4.18
177. SBOH+SBBR=SB2+BROH	5.00E+11	0	37.66
178. SBOH+BR=SBO+HBR	1.00E+13	0	33.47
179. SBOH+CH2BR=SBO+CH3BR	4.00E+12	0	20.92

\* Husain, D.; Slater, N.K.H., Kinetic study of ground state antimony atoms  $Sb(5^4S_{3/2})$  by atomic absorption spectroscopy, J.Photochem, 1977, 7,59-70.

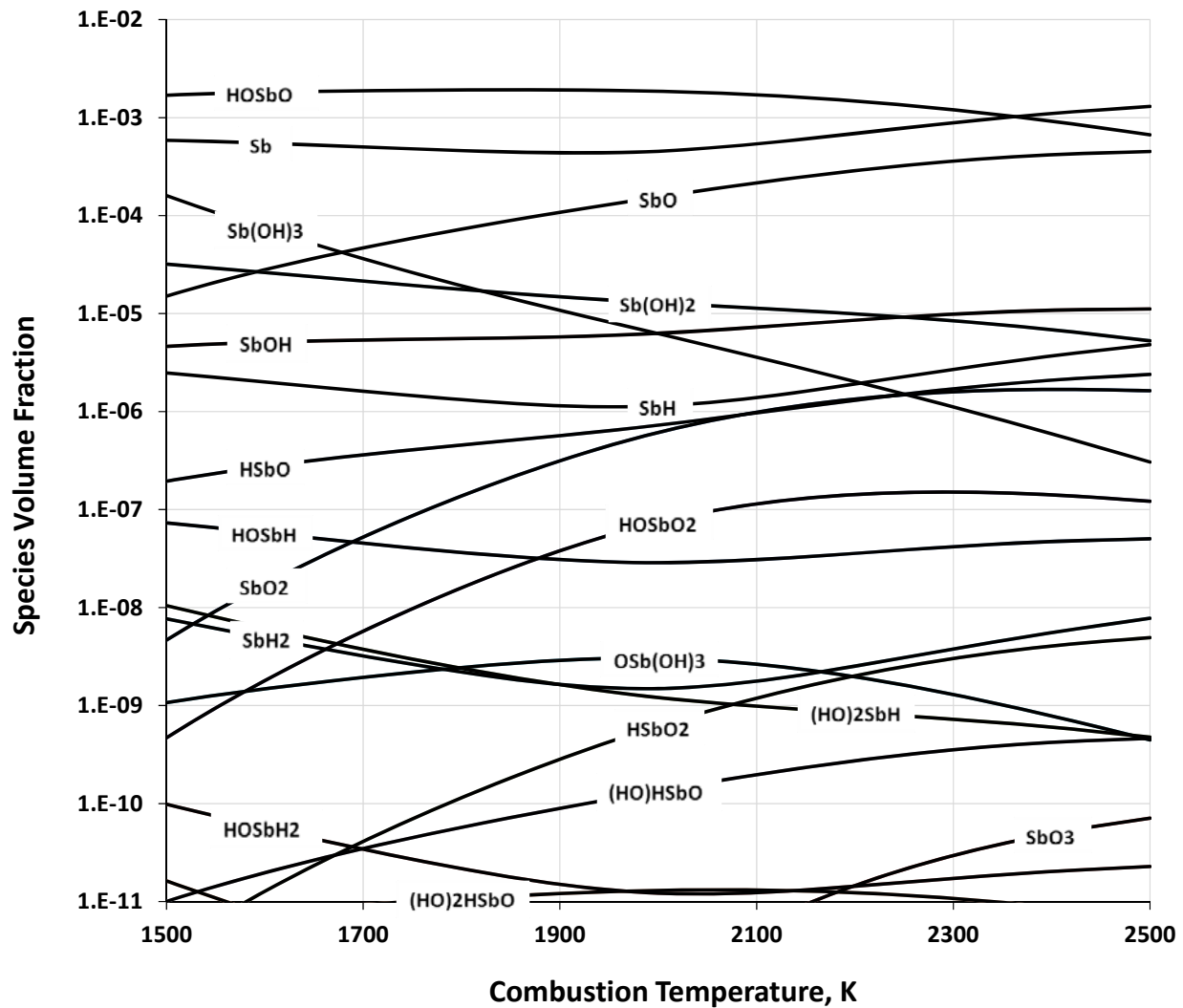


**Figure 1 - Equilibrium concentrations vs. temperature of antimony-containing species in the combustion products of a stoichiometric methane/air flame, with an initial  $\text{SbH}_3$  volume fraction of 0.25 %.**

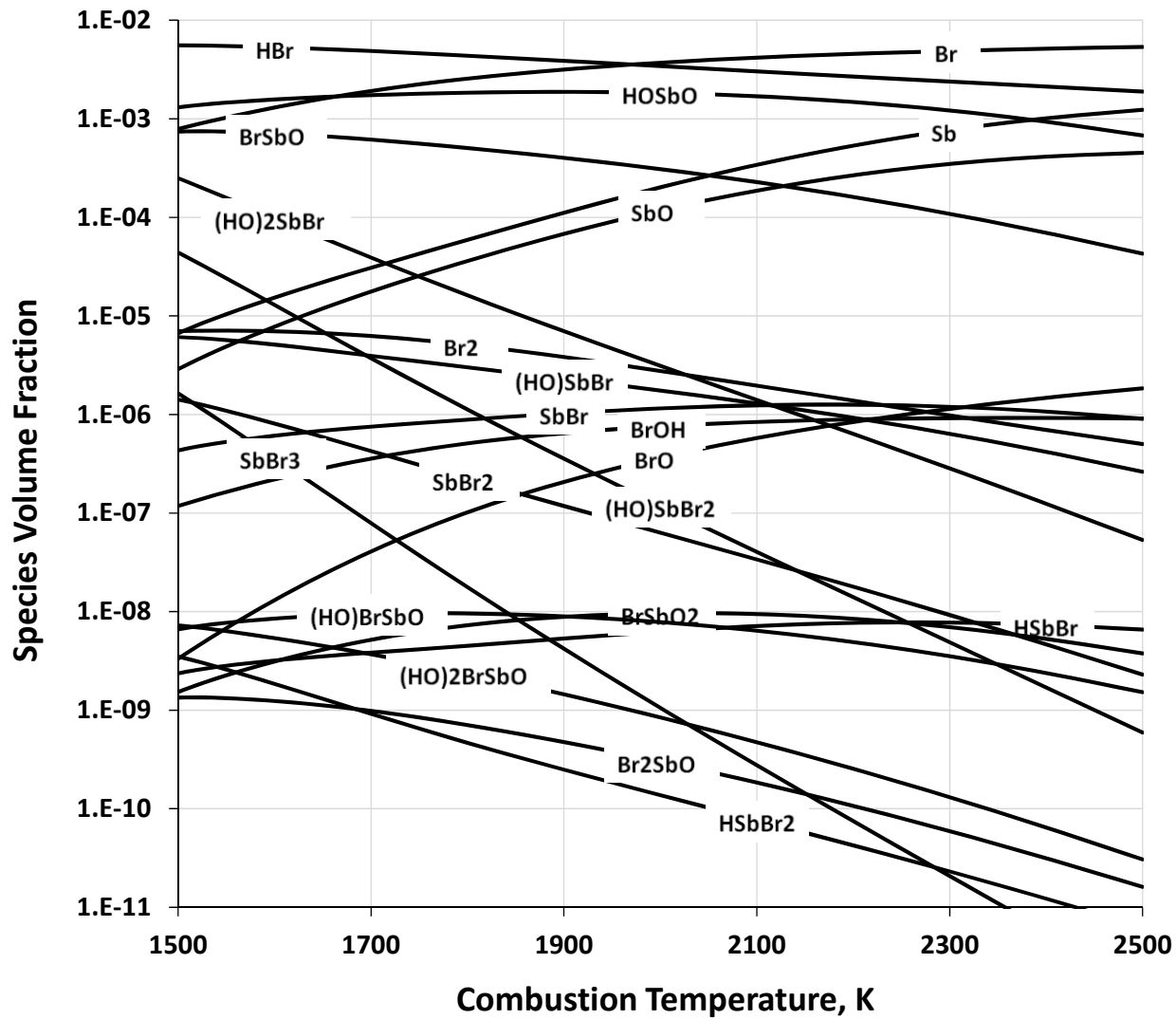


Figure 2 - Equilibrium concentrations of antimony compounds vs. equivalence ratio of methane/air flame with SbBr<sub>3</sub> added at a volume fraction of 0.25 %.

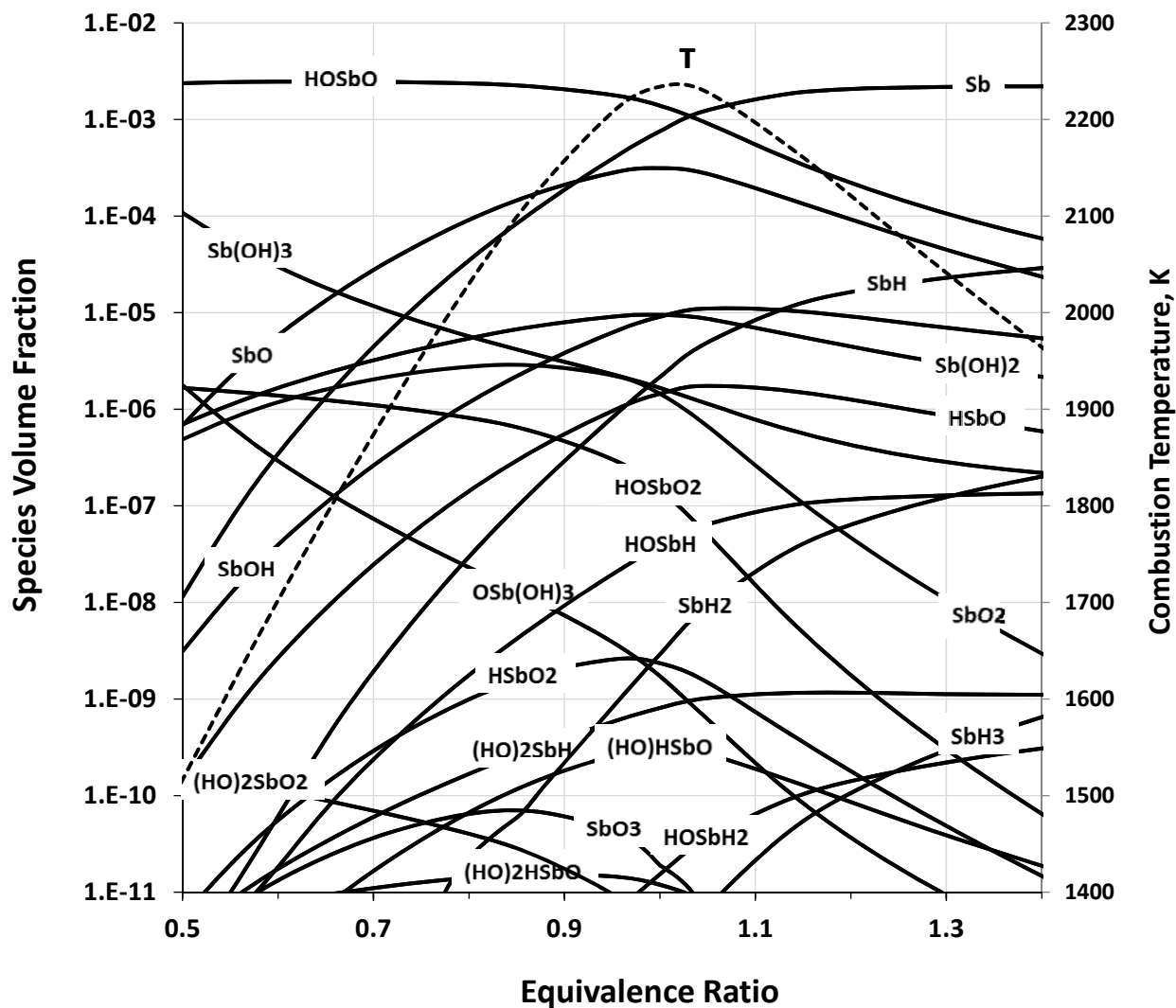


Figure 3 - Equilibrium concentrations of antimony-containing species vs. equivalence ratio of methane/air flame for an initial volume SbBr<sub>3</sub> volume fraction of 0.25 %.

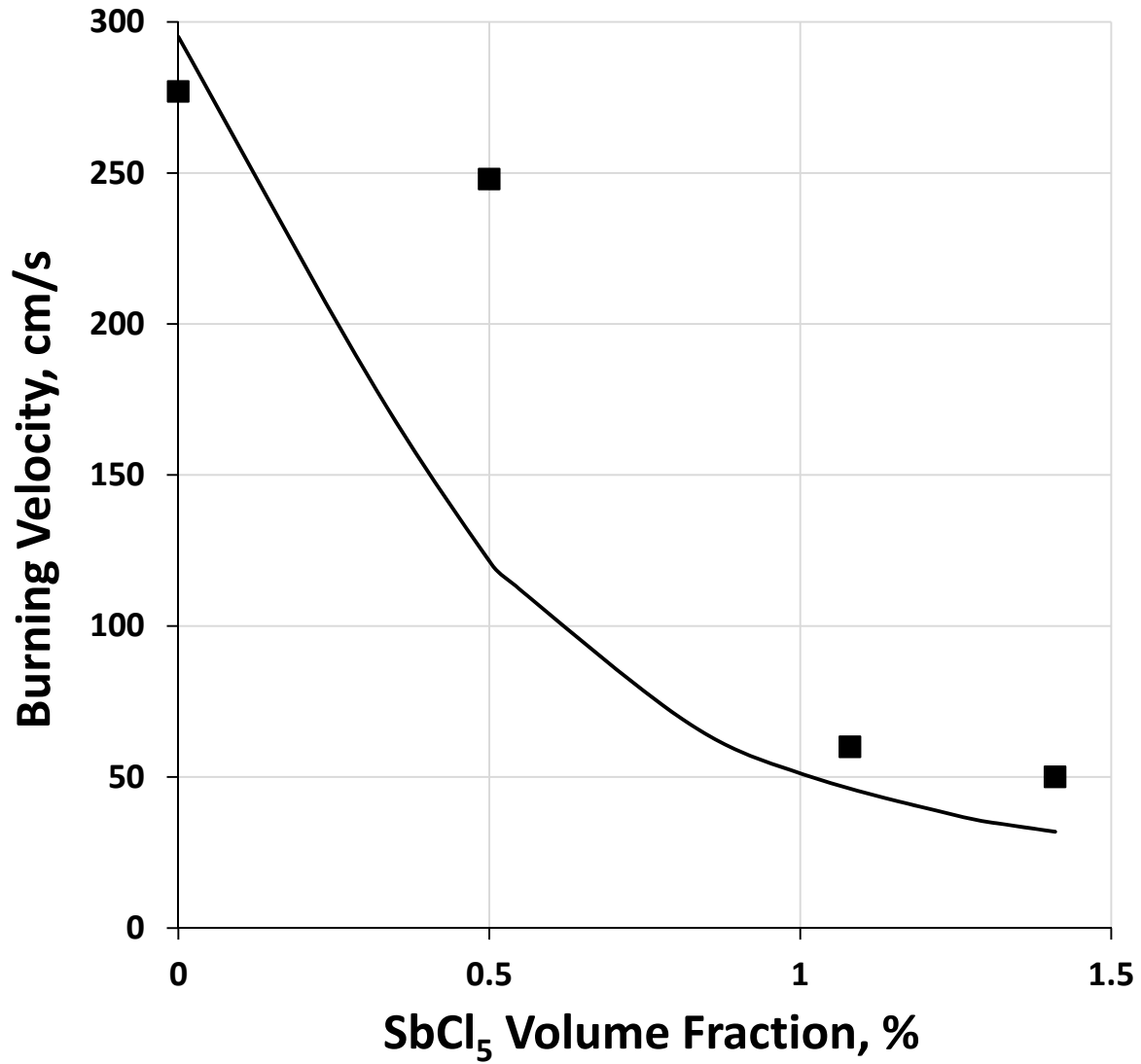


Figure 4 - Laminar burning velocity of hydrogen-air flames (298 K, 1 bar, equivalence ratio 1.75) with added  $\text{SbCl}_5$  (■ – experiment; line: numerical prediction).

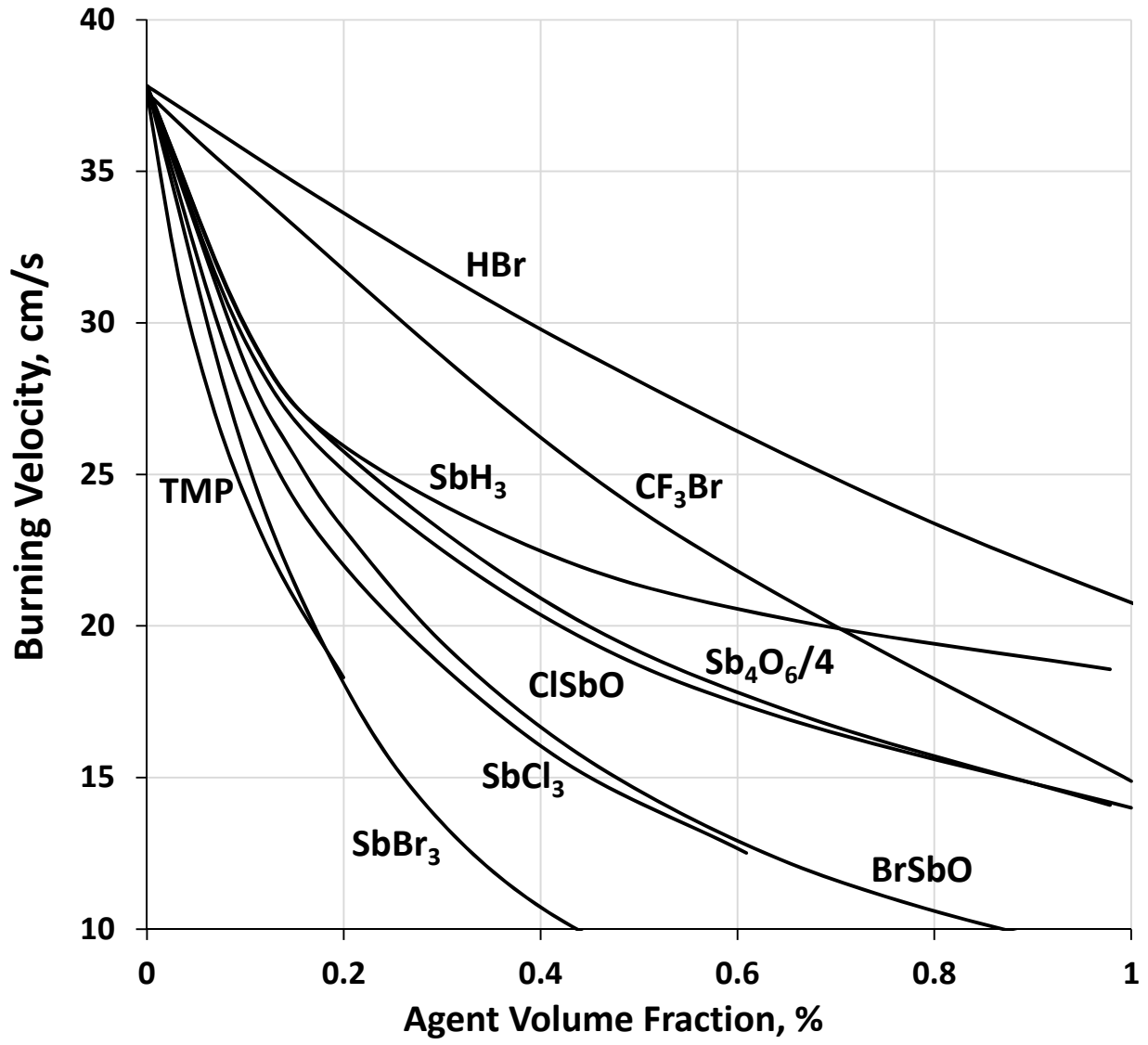


Figure 5 - Laminar burning velocity of stoichiometric methane-air flames (298 K, 1 bar) as a function of inhibitor volume fraction.

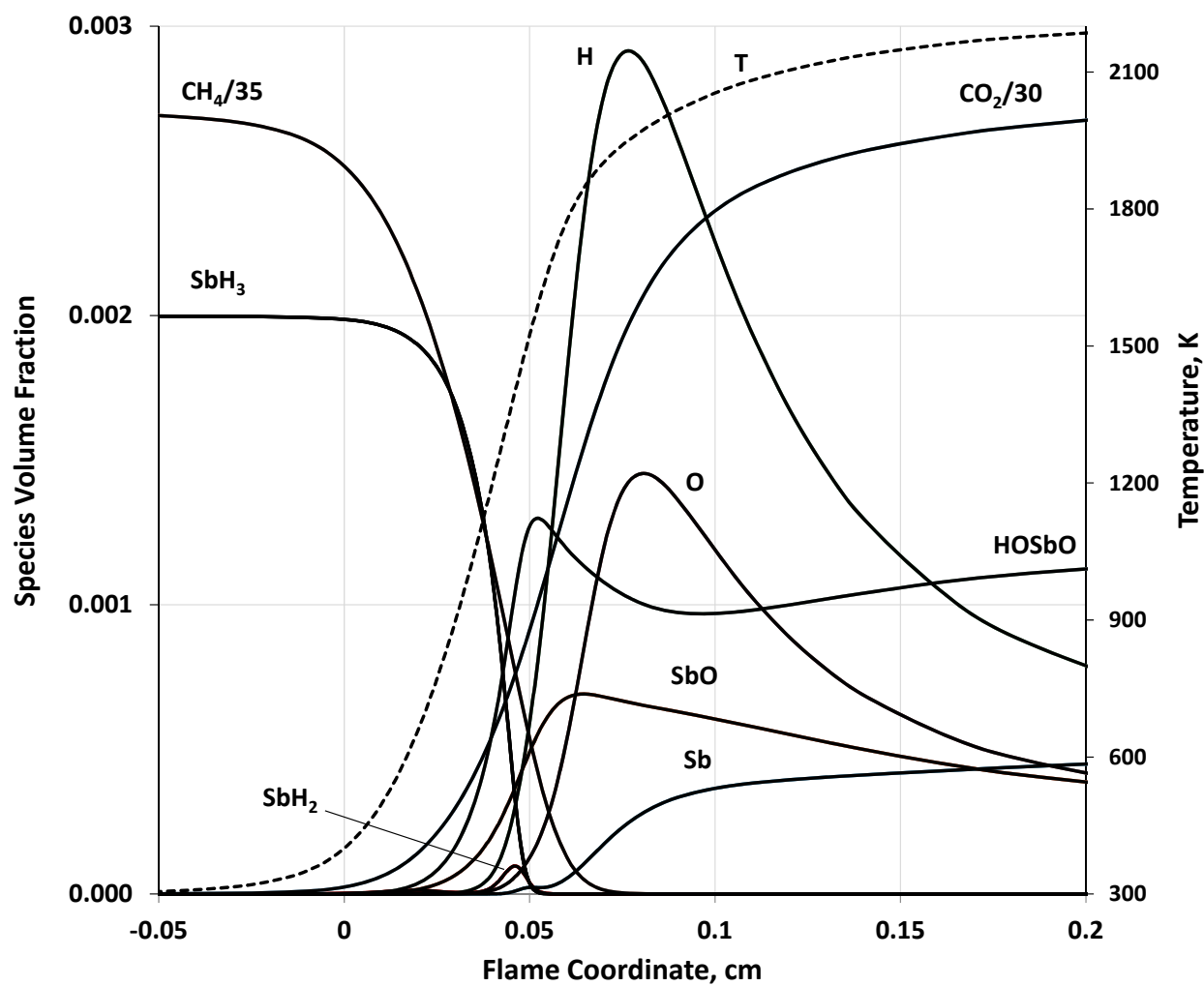
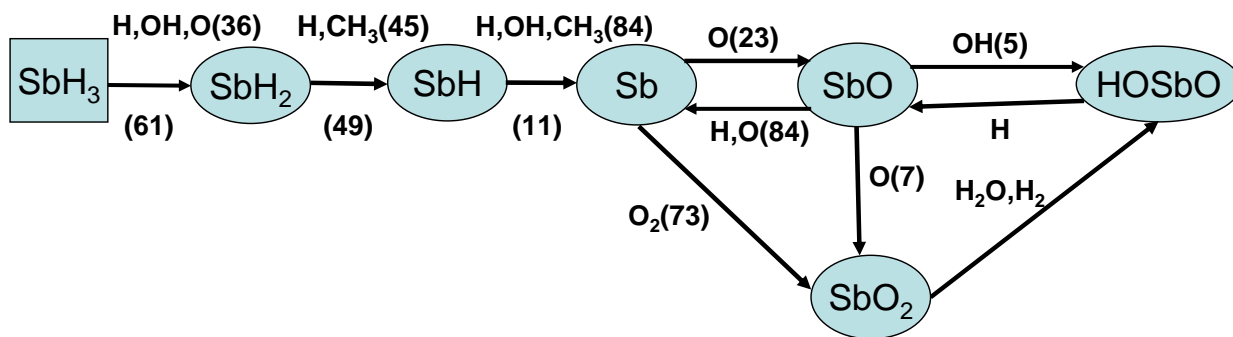


Figure 6 - Flame structure of stoichiometric methane/air flame inhibited by SbH<sub>3</sub> (298K, 1 bar, SbH<sub>3</sub> volume fraction of 0.2 %).



**Figure 7 - The major reaction pathways of antimony-containing species in main reaction zone of a stoichiometric methane/air flame (with an initial SbH<sub>3</sub> volume fraction 0.25 %).**



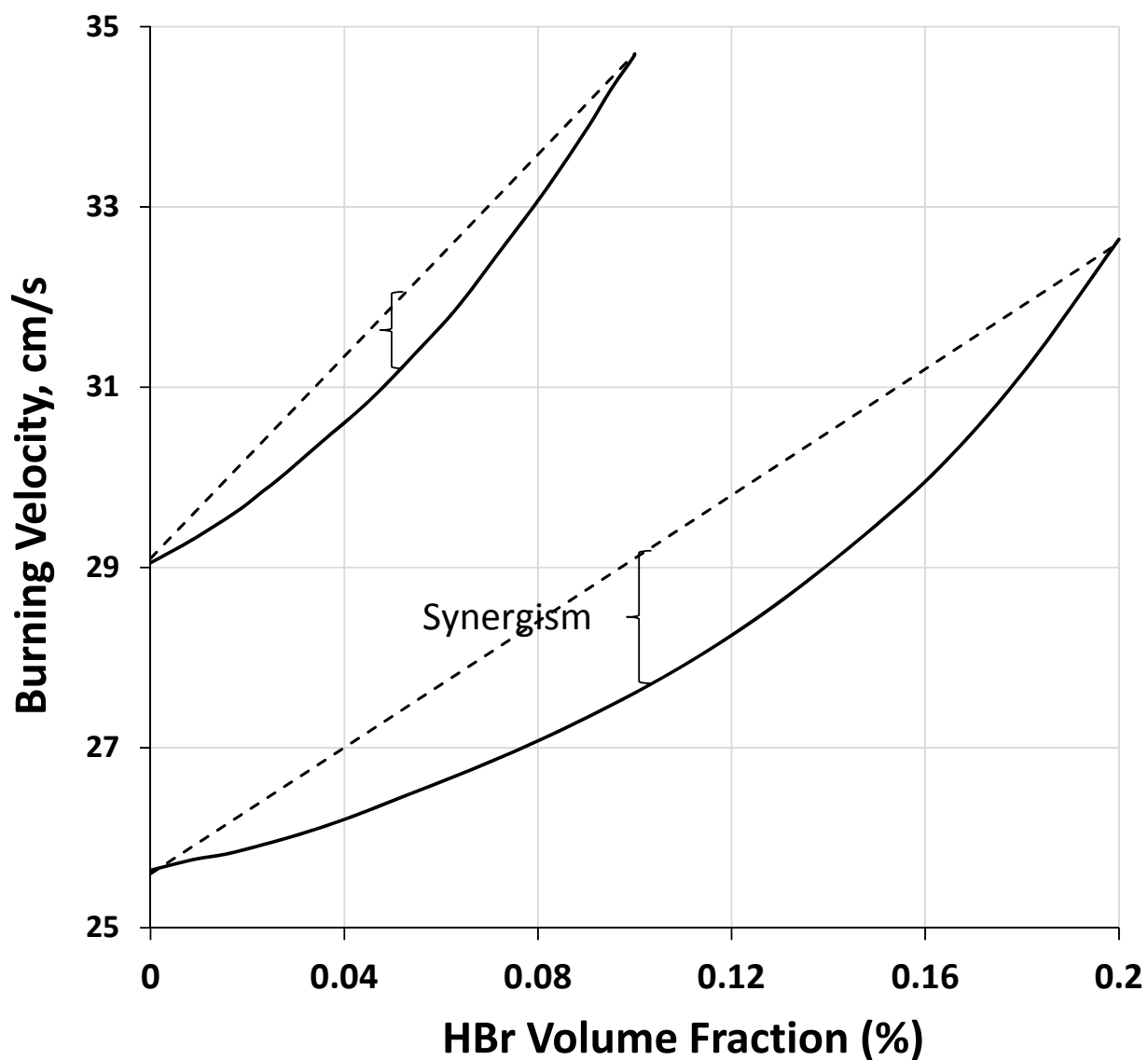


Figure 8 - Burning velocity vs. HBr volume fraction in the reactants (inhibitor is a mixture of  $\text{SbH}_3 + \text{HBr}$ , added at either 0.001 or 0.002 volume fraction, to the stoichiometric methane/air flame (298 K, 1.01 bar).

## Supplemental Material

### 1. Thermodynamic polynomials (Chemkin format) for antimony-containing species

```
SB      GAS      B04/09SB 1.  0.  0.  0. G  298.150 2000.000 1000.  1
  2. 42087320E+00 3. 48363006E-04-4. 87492847E-07 2. 56072866E-10-3. 56862582E-14 2
  3. 10833210E+04 7. 80249403E+00 2. 48973416E+00 7. 79283907E-05-2. 04107407E-07 3
  2. 17573104E-10-7. 89982814E-14 3. 10735029E+04 7. 47922252E+00 3. 18178702E+04 4
SB(CH3)2  T04/09SB 1C  2H  6  OG  200.000 6000.000 1000.  1
  6. 74202280E+00 1. 59118082E-02-5. 63150175E-06 8. 99396716E-10-5. 34173531E-14 2
  1. 42205311E+04-4. 60822517E+00 4. 74741966E+00 1. 27189509E-02 1. 70266233E-05 3
-2. 86489118E-08 1. 20242266E-11 1. 52304029E+04 7. 86382523E+00 1. 73106533E+04 4
SB(CH3) triplet 63005 H  3C  1SB  1  OG  300.000 3000.000 1000.00  1
  0. 29697576E+01 0. 11082103E-01-0. 54282368E-05 0. 12913154E-08-0. 12107738E-12 2
  0. 24777201E+05 0. 12841121E+02 0. 20779578E+01 0. 14966753E-01-0. 11965446E-04 3
  0. 62789806E-08-0. 61471942E-15 0. 24947490E+05 0. 17083682E+02 4
SB(CH3)3  T04/09SB 1. C  3. H  9.  OG  200.000 6000.000 1000.  1
  1. 06182218E+01 2. 18958190E-02-7. 80204951E-06 1. 25201509E-09-7. 46171333E-14 2
-1. 74686603E+02-2. 48860995E+01 6. 79004650E+00 1. 80286318E-02 2. 81660699E-05 3
-4. 64556708E-08 1. 9603118E-11 1. 63764483E+03-1. 51504424E+00 4. 62959333E+03 4
SB(s) REF ELEM B04/09SB 1.  0.  0.  0. S  298.150 904.000 904.  1
  0. 00000000E+00 0. 00000000E+00 0. 00000000E+00 0. 00000000E+00 0. 00000000E+00 2
  0. 00000000E+00 0. 00000000E+00 2. 12273784E+00 6. 03818322E-03-1. 41050855E-05 3
  1. 52517658E-08-5. 38507268E-12-8. 04252525E+02-7. 91696068E+00 0. 00000000E+00 4
SB(l) REF ELEMENT B04/09SB 1.  0.  0.  0. L  904.000 1891.000 1000.  1
  3. 74764275E+00 7. 774849671-05-8. 31208796E-08 3. 86360546E-11-6. 61471942E-15 2
  9. 90188439E+02-1. 38262406E+01 3. 74764275E+00 7. 77484967E-05-8. 31208796E-08 3
  1. 38262406E-11-6. 61471942E-15 9. 90188439E+02-1. 38262406E+01 0. 00000000E+00 4
SB2      T01/09SB 2.  0.  0.  0. G  200.000 6000.000 1000.  1
  4. 44926335E+00 8. 50731434E-05-2. 15467387E-08 3. 72963655E-12-2. 34166278E-16 2
  2. 70431984E+04 5. 37301663E+00 3. 59804769E+00 5. 06905048E-03-1. 10928478E-05 3
  1. 80165334E-08-3. 87449857E-12 2. 71645110E+04 9. 16897750E+00 2. 83841140E+04 4
SBF      T03/09SB 1. F  1.  0.  0. G  200.000 6000.000 1000.  1
  5. 03332293E+00-5. 75565879E-04 3. 29303124E-07-6. 53261567E-11 4. 37256522E-15 2
-1. 04517631E+04-2. 20146752E-01 1. 97345005E+00 1. 34491064E-02-2. 34261965E-05 3
  1. 76006797E-08-4. 87093301E-12-9. 92716684E+03 1. 40999416E+01-8. 91549833E+03 4
SBF3     T03/09SB 1. F  3.  0.  0. G  298.150 4000.000 1000.  1
  8. 87021479E+00 1. 35894382E-03-4. 85074797E-07 7. 63330680E-11-4. 47034933E-15 2
-1. 00544258E+05-1. 47836086E+01 1. 99190356E+00 3. 69570851E-02-7. 05841557E-05 3
  6. 15822022E-08-2. 01310886E-11-9. 94498006E+04 1. 67111795E+01-9. 77247006E+04 4
SBH3     T01/09H  3. SB  1.  0.  0. G  200.000 6000.000 1000.  1
  5. 19970155E+00 4. 67661185E-03-1. 77733186E-06 2. 97629920E-10-1. 82688048E-14 2
  1. 52898503E+04-3. 79348197E+00 3. 19635148E+00 3. 49548430E-03 1. 29554549E-05 3
-1. 84844825E-08 7. 21553443E-12 1. 62216027E+04 8. 31215758E+00 1. 74112966E+04 4
HOSBH    63005H  20  1SB  1  OG  300.000 3000.000 1000.00  1
  0. 55062345E+01 0. 38618323E-02-0. 16928074E-05 0. 36746218E-09-0. 31952322E-13 2
-0. 36915097E+04 0. 12740457E+01 0. 36129284E+01 0. 12138008E-01-0. 15675216E-04 3
  0. 11076976E-07-0. 31419273E-11-0. 33307721E+04 0. 10275225E+02 4
HOSBH2   63005H  30  1SB  1  OG  300.000 3000.000 1000.00  1
  0. 65664142E+01 0. 64704513E-02-0. 31693328E-05 0. 75840330E-09-0. 71668567E-13 2
-0. 11467059E+05-0. 64947408E+01 0. 11231640E+01 0. 30350268E-01-0. 44093326E-04 3
  0. 32739939E-07-0. 95657784E-11-0. 10418949E+05 0. 19401095E+02 4
(HO)2SBH 63005H  30  2SB  1  OG  300.000 3000.000 1000.00  1
  0. 95510723E+01 0. 44967873E-02-0. 16228254E-05 0. 27821056E-09-0. 18096696E-13 2
-0. 44000076E+05-0. 18436842E+02 0. 13631867E+01 0. 41254930E-01-0. 64502959E-04 3
  0. 48515593E-07-0. 13945602E-10-0. 42505062E+05 0. 20207742E+02 4
OSBH2    63005H  20  1SB  1  OG  300.000 3000.000 1000.00  1
  0. 51767448E+01 0. 64813205E-02-0. 36790232E-05 0. 97868610E-09-0. 99971483E-13 2
  0. 20394495E+05 0. 11577140E+01 0. 20823002E+01 0. 18583046E-01-0. 23062058E-04 3
  0. 15817357E-07-0. 45628885E-11 0. 21082004E+05 0. 16292677E+02 4
SBH triplet 63005H  1SB  1  OG  300.000 3000.000 1000.00  1
  0. 28223176E+01 0. 22108686E-02-0. 12400284E-05 0. 32752955E-09-0. 33320693E-13 2
  0. 28713354E+05 0. 93069145E+01 0. 38300626E+01-0. 29123164E-02 0. 81021818E-05 3
-0. 70183160E-08 0. 20857546E-11 0. 28565778E+05 0. 47165849E+01 4
SBH2     63005H  2SB  1  OG  300.000 3000.000 1000.00  1
  0. 30219090E+01 0. 53025317E-02-0. 29993734E-05 0. 79719875E-09-0. 81481891E-13 2
  0. 23800088E+05 0. 94325621E+01 0. 38251193E+01-0. 36711061E-04 0. 79289000E-05 3
-0. 82544608E-08 0. 25779368E-11 0. 23754773E+05 0. 61116533E+01 4
SB406    OSB  40  6  G  300.000 3000.000 1000.00  1
  0. 24589789E+02 0. 47494815E-02-0. 25327138E-05 0. 57598828E-09-0. 44940939E-13 2
```

-0. 15492415E+06-0. 86828366E+02 0. 10674493E+02 0. 63281847E-01-0. 94638035E-04	3
0. 64850717E-07-0. 16831419E-10-0. 15228465E+06-0. 20412902E+02	4
SB203(s1) OSB 20 3 S 300.000 879.000 879.00	1
0. 51026398E+01 0. 44858656E-01-0. 89633694E-04 0. 88201979E-07-0. 31403328E-10	2
-0. 88102849E+05-0. 23556201E+02 0. 51026398E+01 0. 44858656E-01-0. 89633694E-04	3
0. 88201979E-07-0. 31403328E-10-0. 88102849E+05-0. 23556201E+02	4
SB203(s2) OSB 20 3 S 879.000 928.000 928.00	1
0. 37193767E+02-0. 50052660E-01 0. 13804977E-05 0. 65292323E-07-0. 35657030E-10	2
-0. 92917270E+05-0. 18503585E+03 0. 37193767E+02-0. 50052660E-01 0. 13804978E-05	3
0. 65292323E-07-0. 35657030E-10-0. 92917270E+05-0. 18503585E+03	4
SB203(l) OSB 20 3 L 928.000 3000.000 1500.00	1
0. 21649435E+02 0. 00000000E+00 0. 00000000E+00 0. 00000000E+00 0. 00000000E+00	2
-0. 79489385E+05-0. 10689445E+03 0. 21649435E+02 0. 00000000E+00 0. 00000000E+00	3
0. 00000000E+00 0. 00000000E+00-0. 79489385E+05-0. 10689445E+03	4
HOSBO OH 10 2SB 1 G 300.000 3000.000 1000.00	1
0. 66922159E+01 0. 35199344E-02-0. 17559185E-05 0. 44019652E-09-0. 44161519E-13	2
-0. 30306806E+05-0. 29610411E+01 0. 23644721E+01 0. 22996511E-01-0. 34219184E-04	3
0. 24247975E-07-0. 65375063E-11-0. 29549537E+05 0. 17376421E+02	4
HOSBO2 OH 10 3SB 1 G 300.000 3000.000 1000.00	1
0. 89896566E+01 0. 46249570E-02-0. 24616815E-05 0. 64573428E-09-0. 66696994E-13	2
-0. 33392996E+05-0. 12331544E+02 0. 35728917E+01 0. 28234917E-01-0. 40790970E-04	3
0. 28141493E-07-0. 74263616E-11-0. 32406788E+05 0. 13315490E+02	4
OSB(OH)3 OH 30 4SB 1 G 300.000 3000.000 1000.00	1
0. 13546942E+02 0. 80029250E-02-0. 35310995E-05 0. 79287198E-09-0. 72781706E-13	2
-0. 90893276E+05-0. 33443549E+02 0. 46238869E+01 0. 48559205E-01-0. 71661608E-04	3
0. 51077270E-07-0. 13859896E-10-0. 89351868E+05 0. 83890209E+01	4
BR3SBO OBR 30 1SB 1 G 300.000 3000.000 1000.00	1
0. 90206346E+01 0. 16376841E-02-0. 10965824E-05 0. 33124247E-09-0. 37371571E-13	2
-0. 23946925E+05-0. 12139325E+01 0. 66573533E+01 0. 11923680E-01-0. 17774882E-04	3
0. 12282980E-07-0. 32335235E-11-0. 23515912E+05 0. 99793163E+01	4
BR2SBO OBR 20 1SB 1 G 300.000 3000.000 1000.00	1
0. 83257254E+01 0. 11594496E-02-0. 79165486E-06 0. 24253146E-09-0. 27652401E-13	2
-0. 78501404E+04-0. 18076398E+01 0. 64342268E+01 0. 96725199E-02-0. 14981874E-04	3
0. 10649754E-07-0. 28662269E-11-0. 75191945E+04 0. 70809786E+01	4
BR5SBO OBR 10 1SB 1 G 300.000 3000.000 1000.00	1
0. 62486065E+01 0. 12250784E-02-0. 80493231E-06 0. 23967973E-09-0. 26743161E-13	2
-0. 85508315E+04 0. 27436023E+01 0. 46546525E+01 0. 78463013E-02-0. 11104877E-04	3
0. 73517166E-08-0. 18661041E-11-0. 82443110E+04 0. 10372157E+02	4
BR5BO2 OBR 10 2SB 1 G 300.000 3000.000 1000.00	1
0. 85646991E+01 0. 23364779E-02-0. 15332999E-05 0. 45612541E-09-0. 50855512E-13	2
-0. 11543010E+05-0. 74939329E+01 0. 55403556E+01 0. 14853830E-01-0. 20939294E-04	3
0. 13813432E-07-0. 34951767E-11-0. 10959140E+05 0. 69917820E+01	4
H2SBBR OH 2BR 1SB 1 G 300.000 3000.000 1000.00	1
0. 44069287E+01 0. 63327430E-02-0. 36983810E-05 0. 10111142E-08-0. 10586277E-12	2
0. 56346552E+04 0. 86270818E+01 0. 40442866E+01 0. 64699184E-02-0. 19340543E-05	3
-0. 14784967E-08 0. 84488824E-12 0. 57728533E+04 0. 10704969E+02	4
(HO)2BR5BO OH 20 3BR 1SB 1G 300.000 3000.000 1000.00	1
0. 13127475E+02 0. 57253570E-02-0. 26121776E-05 0. 60586247E-09-0. 57181406E-13	2
-0. 68791291E+05-0. 27728281E+02 0. 66508506E+01 0. 34995517E-01-0. 51562913E-04	3
0. 36603350E-07-0. 98974692E-11-0. 67664149E+05 0. 26767704E+01	4
(HO)2HSBO OH 30 3SB 1 G 300.000 3000.000 1000.00	1
0. 99972191E+01 0. 85726928E-02-0. 42416349E-05 0. 10452962E-08-0. 10275489E-12	2
-0. 58616622E+05-0. 17780762E+02 0. 36408416E+01 0. 36990594E-01-0. 51357075E-04	3
0. 35447981E-07-0. 94515240E-11-0. 57494966E+05 0. 12136987E+02	4
(HO)2SBBR OH 20 2SB 1BR 1G 300.000 3000.000 1000.00	1
0. 10901942E+02 0. 45418556E-02-0. 18773908E-05 0. 39711746E-09-0. 34770543E-13	2
-0. 63001920E+05-0. 18788810E+02 0. 52333168E+01 0. 31304336E-01-0. 48153080E-04	3
0. 35335557E-07-0. 97913752E-11-0. 62072594E+05 0. 75370349E+01	4
(HO)2BR5BO OH 20 3SB 1BR 1G 300.000 3000.000 1000.00	1
0. 13127475E+02 0. 57253570E-02-0. 26121776E-05 0. 60586247E-09-0. 57181406E-13	2
-0. 68791291E+05-0. 27728281E+02 0. 66508506E+01 0. 34995517E-01-0. 51562913E-04	3
0. 36603350E-07-0. 98974692E-11-0. 67664149E+05 0. 26767704E+01	4
(HO)2SB02 OH 20 4SB 1 G 300.000 3000.000 1000.00	1
0. 11908105E+02 0. 61269867E-02-0. 28970441E-05 0. 69536309E-09-0. 67568449E-13	2
-0. 54266126E+05-0. 23191822E+02 0. 45838985E+01 0. 39342664E-01-0. 58598839E-04	3
0. 41748745E-07-0. 11310627E-10-0. 52997227E+05 0. 11163527E+02	4
(HO)3SBO OH 30 4SB 1 G 300.000 3000.000 1000.00	1
0. 13546942E+02 0. 80029250E-02-0. 35310995E-05 0. 79287198E-09-0. 72781706E-13	2
-0. 90893276E+05-0. 33443549E+02 0. 46238869E+01 0. 48559205E-01-0. 71661608E-04	3
0. 51077270E-07-0. 13859896E-10-0. 89351868E+05 0. 83890209E+01	4
(HO)BR5BO OH 10 2SB 1BR 1G 300.000 3000.000 1000.00	1
0. 99731874E+01 0. 30890986E-02-0. 14902479E-05 0. 36545427E-09-0. 36217958E-13	2

-0. 28780873E+05-0. 13333367E+02 0. 59809620E+01 0. 21590724E-01-0. 33041773E-04	3
0. 23932529E-07-0. 65611676E-11-0. 28109064E+05 0. 52936322E+01	4
(HO)HSBO OH 20 2SB 1 G 300.000 3000.000 1000.00	1
0. 77520919E+01 0. 61897322E-02-0. 33238851E-05 0. 87220667E-09-0. 89747306E-13	2
-0. 16150882E+05-0. 84591473E+01 0. 32354385E+01 0. 26050079E-01-0. 35805004E-04	3
0. 24320019E-07-0. 64001336E-11-0. 15337238E+05 0. 12882661E+02	4
(HO)(CH3)SBBR OH 40 1SB 1C 1G 300.000 3000.000 1000.00BR	1
0. 71245581E+01 0. 11976996E-01-0. 59571046E-05 0. 14537541E-08-0. 14040846E-12	2
-0. 34562616E+05 0. 13928258E+01 0. 19959884E+01 0. 33358104E-01-0. 39329010E-04	3
0. 24568520E-07-0. 61358073E-11-0. 33580244E+05 0. 25918503E+02	4
(HO)SBBR OH 10 1SB 1BR 1G 300.000 3000.000 1000.00	1
0. 75366101E+01 0. 21259897E-02-0. 84469577E-06 0. 17121481E-09-0. 14404435E-13	2
-0. 17922386E+05-0. 34398613E+01 0. 48081678E+01 0. 15086137E-01-0. 23354483E-04	3
0. 17224118E-07-0. 47892246E-11-0. 17479016E+05 0. 92117009E+01	4
(HO)SBBR2 OH 10 1SB 1BR 2G 300.000 3000.000 1000.00	1
0. 93562426E+01 0. 24473046E-02-0. 10677992E-05 0. 24024225E-09-0. 22326988E-13	2
-0. 41432760E+05-0. 75255722E+01 0. 61043931E+01 0. 17859786E-01-0. 27794146E-04	3
0. 20462890E-07-0. 56792598E-11-0. 40902644E+05 0. 75614514E+01	4
(HO)SBO OH 10 2SB 1 G 300.000 3000.000 1000.00	1
0. 66922159E+01 0. 35199344E-02-0. 17559185E-05 0. 44019652E-09-0. 44161519E-13	2
-0. 30306806E+05-0. 29610411E+01 0. 23644721E+01 0. 22996511E-01-0. 34219184E-04	3
0. 24247975E-07-0. 65375063E-11-0. 29549537E+05 0. 17376421E+02	4
(HO)SBO2 OH 10 3SB 1 G 300.000 3000.000 1000.00	1
0. 89896566E+01 0. 46249570E-02-0. 24616815E-05 0. 64573428E-09-0. 66696994E-13	2
-0. 33392996E+05-0. 12331544E+02 0. 35728917E+01 0. 28234917E-01-0. 40790970E-04	3
0. 28141493E-07-0. 74263616E-11-0. 32406788E+05 0. 13315490E+02	4
HSBBR OH 1BR 1SB 1 G 300.000 3000.000 1000.00	1
0. 47905847E+01 0. 30746979E-02-0. 18120556E-05 0. 49951176E-09-0. 52678010E-13	2
0. 14283639E+05 0. 69967429E+01 0. 44532155E+01 0. 41653477E-02-0. 30597896E-05	3
0. 10725073E-08-0. 13122013E-12 0. 14364054E+05 0. 86890612E+01	4
HSBBR2 OH 1BR 2SB 1 G 300.000 3000.000 1000.00	1
0. 63114149E+01 0. 38987785E-02-0. 23747212E-05 0. 67187981E-09-0. 72329256E-13	2
-0. 63087434E+04 0. 48784322E+01 0. 46190271E+01 0. 11079863E-01-0. 13763649E-04	3
0. 86760318E-08-0. 21762506E-11-0. 59908425E+04 0. 12940342E+02	4
HSBO OH 10 1SB 1 G 300.000 3000.000 1000.00	1
0. 43249036E+01 0. 38855506E-02-0. 23541319E-05 0. 66084305E-09-0. 70549134E-13	2
0. 92983775E+04 0. 63149527E+01 0. 28671228E+01 0. 86390978E-02-0. 78680889E-05	3
0. 32592385E-08-0. 45075403E-12 0. 96438124E+04 0. 13617296E+02	4
HSBO2 OH 10 2SB 1 G 300.000 3000.000 1000.00	1
0. 64474457E+01 0. 52659794E-02-0. 32463687E-05 0. 92452434E-09-0. 99874002E-13	2
0. 19208840E+02-0. 21247668E+01 0. 33513262E+01 0. 17255357E-01-0. 20637786E-04	3
0. 12123702E-07-0. 28008935E-11 0. 65818773E+03 0. 12910995E+02	4
(CH3)2SBBR OH 6BR 1SB 1C 2G 300.000 3000.000 1000.00	1
0. 33390036E+01 0. 19747229E-01-0. 93226638E-05 0. 21504051E-08-0. 19653412E-12	2
-0. 76162709E+04 0. 22132582E+02 0. 56300836E+00 0. 33135291E-01-0. 32830880E-04	3
0. 20106631E-07-0. 52566109E-11-0. 71752760E+04 0. 34954134E+02	4
(CH30)SBO OH 30 2SB 1C 1G 300.000 3000.000 1000.00	1
0. 51744657E+01 0. 13589945E-01-0. 69103373E-05 0. 16996246E-08-0. 16398752E-12	2
-0. 26441909E+05 0. 77395613E+01 0. 38035445E+01 0. 17199160E-01-0. 95124539E-05	3
0. 15598989E-08 0. 33956143E-12-0. 26074002E+05 0. 14822081E+02	4
(CH30)SBO2 OH 30 3SB 1C 1G 300.000 3000.000 1000.00	1
0. 75978840E+01 0. 14455777E-01-0. 74613300E-05 0. 18617147E-08-0. 18200026E-12	2
-0. 29405786E+05-0. 58102384E+01 0. 48058834E+01 0. 23932985E-01-0. 19140949E-04	3
0. 79573327E-08-0. 12832061E-11-0. 28762846E+05 0. 80822497E+01	4
CH3SBBR OH 3C 1SB 1BR 1G 300.000 3000.000 1000.00	1
0. 47737947E+01 0. 81694213E-02-0. 41195057E-05 0. 10108226E-08-0. 97681915E-13	2
0. 80613140E+04 0. 11623783E+02 0. 28138346E+01 0. 16639769E-01-0. 17770789E-04	3
0. 10742185E-07-0. 26881495E-11 0. 84217806E+04 0. 20921831E+02	4
CH3SBBR2 OH 3C 1SB 1BR 2G 300.000 3000.000 1000.00	1
0. 71486110E+01 0. 89501987E-02-0. 50599469E-05 0. 13555426E-08-0. 14005275E-12	2
-0. 14734692E+05 0. 39044471E+01 0. 38553074E+01 0. 19961747E-01-0. 18334771E-04	3
0. 80437593E-08-0. 12716904E-11-0. 13967948E+05 0. 20333150E+02	4
CH3SBO2 OH 30 2SB 1C 1G 300.000 3000.000 1000.00	1
0. 75580475E+01 0. 99368574E-02-0. 52204933E-05 0. 13299830E-08-0. 13277433E-12	2
-0. 90381881E+04-0. 25478572E+01 0. 28850746E+01 0. 29108072E-01-0. 34696298E-04	3
0. 21459842E-07-0. 52850698E-11-0. 81275597E+04 0. 19876705E+02	4
SBBR OBR 1SB 1 G 300.000 3000.000 1000.00	1
0. 44043655E+01 0. 17355236E-03-0. 12287420E-06 0. 38616878E-10-0. 44858548E-14	2
0. 21019163E+05 0. 71538896E+01 0. 40770664E+01 0. 17341508E-02-0. 28408752E-05	3
0. 21020198E-08-0. 58318713E-12 0. 21072053E+05 0. 86700678E+01	4
SBBR2 OBR 2SB 1 G 300.000 3000.000 1000.00	1
0. 58172539E+01 0. 33188141E-03-0. 23508292E-06 0. 73906183E-10-0. 85872063E-14	2

0. 18174069E+04	0. 78061678E+01	0. 51904986E+01	0. 33225329E-02-0.	54465052E-05	3
0. 40318178E-08-0.	11189726E-11	0. 19185764E+04	0. 10708993E+02		4
SBBR3	OBR 3SB 1	G	300.000	3000.000 1000.00	1
0. 77163181E+01	0. 51563412E-03-0.	36544698E-06	0. 11493506E-09-0.	13358105E-13	2
-0. 19141187E+05	0. 31637587E+01	0. 67410205E+01	0. 51734925E-02-0.	84872364E-05	3
0. 62861292E-08-0.	17453236E-11-0.	18983961E+05	0. 76798390E+01		4
SBO	OO 1SB 1	G	300.000	3000.000 1000.00	1
0. 38993692E+01	0. 96143474E-03-0.	62265889E-06	0. 18331443E-09-0.	20270745E-13	2
0. 15315593E+05	0. 68091294E+01	0. 27398060E+01	0. 55649946E-02-0.	74759595E-05	3
0. 47174887E-08-0.	11451411E-11	0. 15549240E+05	0. 12412024E+02		4
SBO2	OO 2SB 1	G	300.000	3000.000 1000.00	1
0. 44373834E+01	0. 11426936E-03-0.	81196127E-07	0. 25581985E-10-0.	29770086E-14	2
0. 21924466E+04	0. 99553144E+01	0. 42196614E+01	0. 11582053E-02-0.	19066715E-05	3
0. 14156133E-08-0.	39374678E-12	0. 22273386E+04	0. 10962435E+02		4
SBO3	OO 3SB 1	G	300.000	3000.000 1000.00	1
0. 80354039E+01	0. 16259181E-02-0.	10943742E-05	0. 33175783E-09-0.	37525788E-13	2
0. 93571376E+04-0.	59190868E+01	0. 55363783E+01	0. 12553130E-01-0.	18881858E-04	3
0. 13121190E-07-0.	34676613E-11	0. 98103872E+04	0. 59044897E+01		4
SBOH	OH 10 1SB 1	G	300.000	3000.000 1000.00	1
0. 47522135E+01	0. 17412028E-02-0.	57729000E-06	0. 88436902E-10-0.	49001931E-14	2
0. 37155454E+04	0. 41506999E+01	0. 26484993E+01	0. 11765773E-01-0.	18028715E-04	3
0. 13332434E-07-0.	37183277E-11	0. 40558026E+04	0. 13897476E+02		4
SB(OH)2	OH 20 2SB 1	G	300.000	3000.000 1000.00	1
0. 82615074E+01	0. 39224265E-02-0.	14583960E-05	0. 27002656E-09-0.	20402408E-13	2
-0. 36810705E+05-0.	93188910E+01	0. 34335647E+01	0. 26896231E-01-0.	41412152E-04	3
0. 30567897E-07-0.	85103784E-11-0.	36028218E+05	0. 13057633E+02		4
SB(OH)3	OH 30 3SB 1	G	300.000	3000.000 1000.00	1
0. 11464167E+02	0. 66354891E-02-0.	26944180E-05	0. 55756429E-09-0.	47711331E-13	2
-0. 83821828E+05-0.	25800188E+02	0. 33318789E+01	0. 45107417E-01-0.	69316474E-04	3
0. 50915044E-07-0.	14122775E-10-0.	82492509E+05	0. 11947706E+02		4
CLSBO	OCL 10 1SB 1	G	300.000	3000.000 1000.00	1
0. 62486065E+01	0. 12250784E-02-0.	80493231E-06	0. 23967973E-09-0.	26743161E-13	2
-0. 14790877E+05-0.	24159838E-01	0. 46546525E+01	0. 78463013E-02-0.	11104877E-04	3
0. 73517166E-08-0.	18661041E-11-0.	14484357E+05	0. 76043950E+01		4
SBCL2	T02/09SB 1. CL 2.	0. G	200.000	6000.000 1000.	1
5. 93482013E+00	1. 08999381E-03-4.	26609277E-07	7. 27977714E-11-4.	52597505E-15	2
-1. 38933126E+04-8.	23285793E-01	3. 26046441E+00	8. 13468529E-03-5.	31503869E-06	3
-1. 00841552E-09	1. 59478097E-12-1.	31613843E+04	1. 30106100E+01-1.	18759133E+04	4
SBCL3	T02/09SB 1. CL 3.	0. G	200.000	6000.000 1000.	1
9. 72981943E+00	2. 86438114E-04-1.	14493259E-07	1. 98078808E-11-1.	24319722E-15	2
-4. 06639954E+04-1.	46490216E+01	5. 51759463E+00	2. 44777531E-02-5.	31507818E-05	3
5. 13625769E-08-1.	82868138E-11-4.	00472434E+04	4. 23196216E+00-3.	76909283E+04	4
SBCL5	T03/09SB 1. CL 5.	0. G	200.000	6000.000 1000.	1
1. 54869771E+01	5. 43850014E-04-2.	17373802E-07	3. 76055163E-11-2.	36017400E-15	2
-5. 68371308E+04-3.	79009433E+01	7. 49842062E+00	4. 64325927E-02-1.	00842443E-04	3
9. 74659896E-08-3.	47058612E-11-5.	56676517E+04	-2. 09441114E+00-5.	20829249E+04	4
SBCL triplet 63005	CL 1SB 1	0 OG	300.000	3000.000 1000.00	1
0. 44258150E+01	0. 98458925E-04-0.	52892768E-07	0. 13053074E-10-0.	12234332E-14	2
0. 10023765E+05	0. 56614704E+01	0. 37460264E+01	0. 32781339E-02-0.	57973080E-05	3
0. 46820131E-08-0.	14256546E-11	0. 10146168E+05	0. 88496041E+01		4
SBCL4	OCL 4SB 1	G	300.000	3000.000 1000.00	1
0. 90206346E+01	0. 16376841E-02-0.	10965824E-05	0. 33124247E-09-0.	37371571E-13	2
-0. 37785735E+05-0.	29400096E+01	0. 66573533E+01	0. 11923680E-01-0.	17774882E-04	3
0. 12282980E-07-0.	32335235E-11-0.	37354723E+05	0. 82532392E+01		4

## 2. Kinetic sub-model for SbCl5 and SbCl3

1. SBCL5=SBCL4+CL	5. 50E+15	0. 0	67000. 0
2. SBCL4=SBCL3+CL	2. 00E+15	0. 0	30000. 0
3. SBCL3=SBCL2+CL	2. 00E+16	0. 0	85000. 0
4. SBCL2=SBCL+CL	2. 00E+15	0. 0	79000. 0
5. SBCL=SB+CL	3. 00E+15	0. 0	75000. 0
6. SBCL5+H=SBCL4+HCL	2. 00E+13	0. 0	2000. 0
7. SBCL5+OH=SBCL4+HOCL	2. 30E+13	0. 0	17000. 0
8. SBCL5+O=SBCL4+CLO	1. 80E+13	0. 0	11000. 0
9. SBCL5+CL=SBCL4+CL2	4. 00E+12	0. 0	15000. 0
10. SBCL4+H=SBCL3+HCL	1. 00E+13	0. 0	0. 0
11. SBCL4+OH=SBCL3+HOCL	5. 00E+13	0. 0	4000. 0
12. SBCL4+O=SBCL3+CLO	2. 20E+13	0. 0	1500. 0

13.	SBCL3+H=SBCL2+HCL	2.00E+13	0.0	5500.0
14.	SBCL3+O=SBCL2+CL0	2.20E+13	0.0	19000.0
15.	SBCL3+CL=SBCL2+CL2	1.00E+13	0.0	27000.0
16.	SBCL3+CH3=SBCL2+CH3CL	8.00E+12	0.0	9500.0
17.	SBCL2+H=SBCL+HCL	5.40E+13	0.0	5000.0
18.	SBCL2+OH=SBCL+HOCL	1.50E+13	0.0	5500.0
19.	SBCL2+O=SBCL+CL0	1.80E+13	0.0	20000.0
20.	SBCL2+CL=SBCL+CL2	8.00E+12	0.0	21000.0
21.	SBCL+H=SB+HCL	3.00E+13	0.0	4500.0
22.	SBCL+OH=SB+HOCL	1.50E+13	0.0	23000.0
23.	SBCL+O=SB+CL0	4.00E+13	0.0	15000.0
24.	SBCL+CL=SB+CL2	7.00E+12	0.0	20500.0
25.	SBCL+H=SBH+CL	5.00E+12	0.0	15500.0
26.	SBCL+OH=SB0+HCL	5.90E+12	0.0	6500.0
27.	SBCL+O=SB0+CL	7.20E+13	0.0	6500.0
28.	CLSBO+H=SB0+HCL	1.50E+13	0.0	7500.0
29.	CLSBO+O=SBCL+O2	3.50E+12	0.0	9000.0
30.	SBCL+O+M=CLSBO+M	2.00E+16	0.0	0.0
31.	SB0+CL+M=CLSBO+M	1.00E+16	0.0	0.0
32.	SBCL+OH=CLSBO+H	2.00E+12	0.0	11000.0
33.	SBCL+CH30=CLSBO+CH3	2.30E+12	0.0	8000.0
34.	SBCL+SB0=CLSBO+SB	8.00E+11	0.0	7500.0
35.	SBCL+SB02=CLSBO+SB0	1.50E+12	0.0	7000.0
36.	SB0+CL2=CLSBO+CL	1.00E+13	0.0	5500.0